Table 1 Association of cancer stem cell (CSC) marker staining with clinicopathologic features of gastric cancer (GC)

Total	ALDH1 104/190 (55%)		CD44 117/190 (62%)		CD133 18/190 (9%)	
% positive cells in stained case	10–90%		10–90%		10–40%	
Characters	Positive rate	*P*-value*	Positive rate	*P*-value*	Positive rate	*P*-value*
T grade†						
T1	19/45 (42%)	0.02	25/45 (56%)	0.36	4/45 (9%)	0.92
T2/3/4	85/145 (58%)		92/145 (63%)		14/145 (9%)	
N grade†						
N0	49/80 (61%)	0.14	42/80 (53%)	0.04	3/80 (4%)	0.02
N1/2/3	55/110 (50%)		75/110 (68%)		15/110 (14%)	
TNM stage†						
Stage I/II	29/69 (42%)	0.01	32/69 (46%)	<0.001	4/69 (5%)	0.24
Stage III/IV	75/121 (61%)		85/121 (70%)		14/121 (11%)	
Histology‡						
Intestinal	57/72 (79%)	<0.001§	47/72 (47%)	0.43§	13/72 (18%)	<0.001§
Diffuse	37/94 (39%)		57/94 (60%)		4/94 (4%)	
Mixed	10/24 (41%)		13/24 (54%)		1/24 (4%)	

*χ^2 test: $P < 0.05$ was considered significant.

†Tumor stage was classified according to the criteria of the International Union Against Cancer Tumor Node Metastasis (TNM) classification of malignant tumors.

‡Histology was according to the Lauren classification.

§Intestinal versus Diffuse plus Mixed-type.

ALDH1, aldehyde dehydrogenase 1.

were estimated from Cox proportional hazard models. For all analyses, age was treated as a categorical variable (65 years old plus, more than 65 years old, versus less than 65 years old). For final multivariable Cox regression models, all variables were included that were moderately associated with cancer-specific mortality ($P < 0.10$). All *P*-values were two-sided, and the significance level was set at $P < 0.05$.

RESULTS

Expression of CSC markers (ALDH1, CD44, CD133) in non-neoplastic gastric mucosa and GC

We examined the expression of ALDH1, CD44, and CD133 by immunohistochemical staining in normal gastric mucosa, intestinal metaplasia, and a series of 190 specimens of GC. In normal gastric mucosa, staining of ALDH1 was detected in the cytoplasm of parietal cells. CD44 was detected in lymphocytes and stromal cells but not epithelial cells; this is consistent with a previous report.[28] CD133 staining was not detected in normal gastric epithelial and stromal cells. Although stem cells of normal gastric gland are considered to be located in the gastric isthmus; no staining of these three molecules was observed in this region. In intestinal metaplasia, CD44 and ALDH1 expression were found in the basal lesion of the metaplastic gland (data not shown). This expression pattern mimics that of the normal colon as per previous reports.[20,29] CD133 staining was not detected in metaplastic lesions.

Out of 190 cases of GC, 104 (55%) were positive for ALDH1, 117 (62%) were positive for CD44, and 18 (9%) were positive for CD133 (Table 1). ALDH1 and CD44 were also observed mainly in the cytoplasm and the membrane of the tumor cells, respectively. Many tumor cells were positive for ALDH1 and CD44 in both intestinal-type and diffuse-type GC (Fig. 1a, b, d and e). CD133 was expressed in the apical membrane of the tumor cells. CD133-positive staining was observed in intestinal-type and diffuse-type GC with partial glandular formation (Fig. 1c,f). In GC, the percentage of ALDH1- and CD44-stained tumor cells ranged from 0% to 90%, and the percentage of CD133-stained tumor cells ranged from 0% to 40% (Table 1). More than half of ALDH1- and CD44-positive cases contained over 50% positive cancer cells. CD44 expression was detected in whole tumor lesions. Most CD133-positive cases included less than 20% positive cancer cells. For each CSC marker, immunostaining was considered positive when at least 10% of tumor cells were stained, on the basis of previous reports.[25–27]

Correlation between CSC markers and clinicopathologic features

The relationship of CSC marker staining to clinicopathologic characteristics was investigated (Table 1). ALDH1-positive GC cases showed more advanced T stage ($P = 0.02$, χ^2 test), TNM stage ($P = 0.01$, χ^2 test), and tended to be intestinal histology ($P < 0.001$, χ^2 test) than ALDH1-negative cases. CD44-positive GC cases showed more advanced N stage

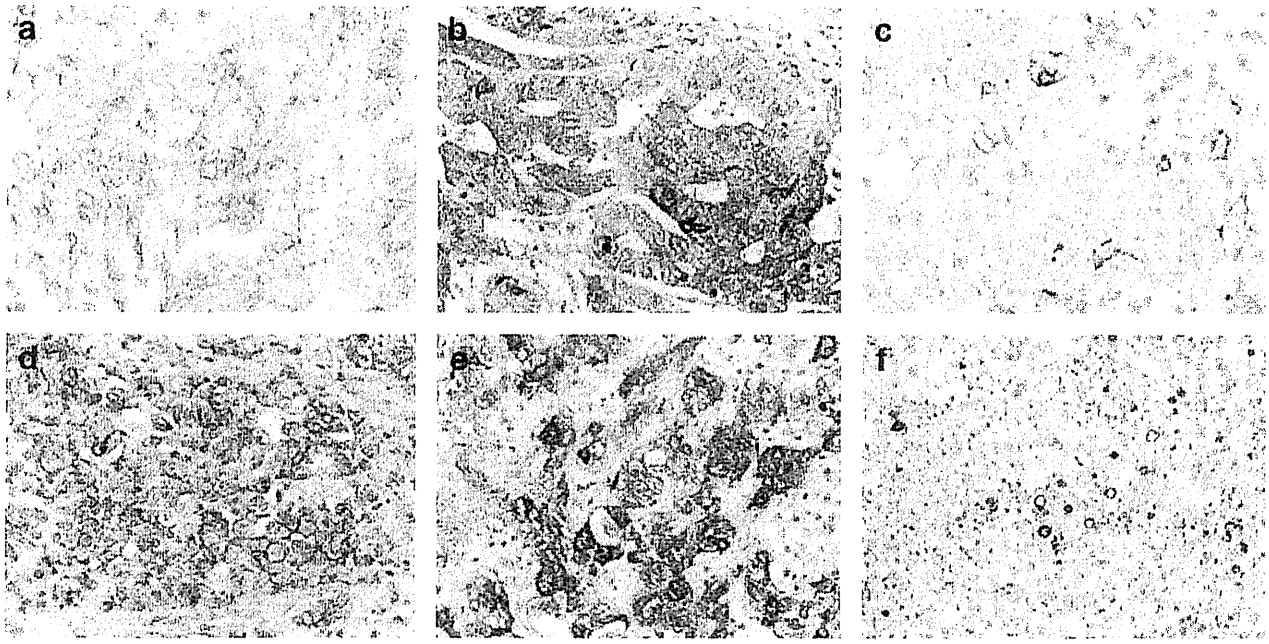

Figure 1 Immunohistochemical analysis of cancer stem cell (CSC) makers in gastric cancer (GC) tissue. Membranous staining of CD44 was observed in intestinal-type (a) and diffuse-type (d) GC (Original magnification: ×400). cytoplasmic staining of aldehyde dehydrogenase 1 (ALDH1) was observed in intestinal-type (b) and diffuse-type (e) GC (Original magnification: ×400). Staining of CD133 was observed in apical membranes in intestinal-type GC (c) and diffuse-type GC with partial glandular formation (f) (Original magnification: ×400).

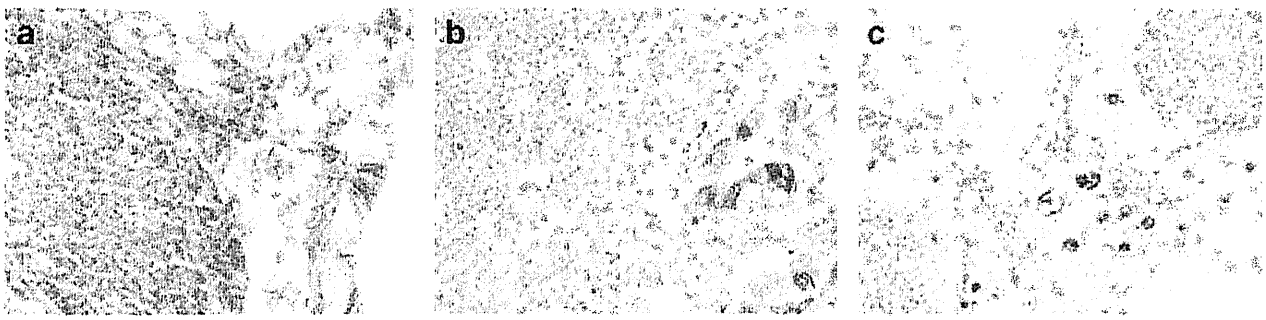

Figure 3 Immunohistochemical analysis of cancer stem cell (CSC) markers in lymph node metastasis of gastric cancer (GC). Expression pattern of CD44 (a), aldehyde dehydrogenase 1 (ALDH1) (b), and CD133 (c) in GC lymph node metastasis of (Original magnification: ×400). The staining patterns of all molecules were similar to those of the primary site.

(P = 0.04, χ^2 test) and TNM stage ($P < 0.001$, χ^2 test) than CD44-negative cases. CD133-positive GC cases also showed more advanced N stage (P = 0.02, χ^2 test) and tended to be intestinal-type in histological character (P = 0.03, χ^2 test).

Correlation between 5 year overall survival and the CSC marker expression

The relationship between survival probability and CSC marker staining was examined in 96 GC cases. The 5 year overall survival rate was 48% for CD44-positive cases and 62% for CD44-negative cases. The 5 year overall survival rate was 35% for ALDH1-positive cases and 46% for ALDH1-negative cases. For CD133, the 5 year overall survival rate was 0% for positive cases and 52% negative cases. CD44-positive patients had significantly lower survival probability than CD44-negative patients ($P < 0.001$; Fig. 2a). Moreover, CD133-positive cases had a shorter overall survival time than CD133-negative cases ($P = 0.006$; Fig. 2b), whereas staining with ALDH1 had no prognostic impact ($P = 0.94$; Fig. 2c). We also investigated the relationship between survival probability and CSC marker staining in 59 cases of advanced GC (more

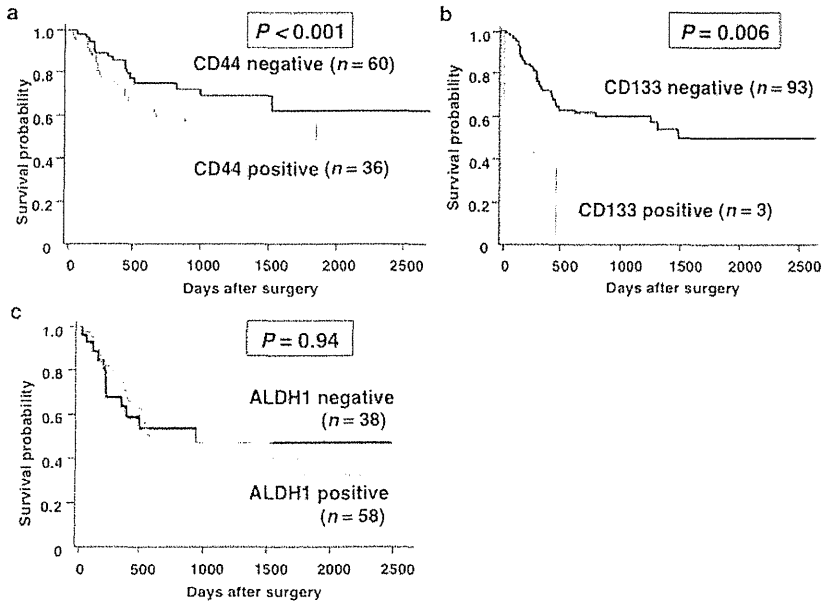

Figure 2 Survival of patients with gastric cancer (GC). (a) Kaplan–Meier curves of patients with CD44-negative or CD44-positive GC. (b) Kaplan–Meier curves of patients with CD133-negative or CD133-positive GC. (c) Kaplan–Meier curves of patients with aldehyde dehydrogenase 1 (ALDH1)- negative or ALDH1-positive GC.

than stage II) and 38 cases of stage II and III, and obtained comparable results were obtained (advanced cases; CD133: $P < 0.001$, CD44: $P = 0.02$, ALDH1: $P = 0.56$, stage II and III cases; CD133: $P < 0.001$, CD44: $P = 0.006$, ALDH1: $P = 0.27$, log-rank test). In addition, because it is well-known that tumors displaying different histological types are associated with distinct biological behavior, we examined the relationship between survival and CSC marker staining in 42 cases of intestinal-type GC and 45 cases of diffuse-type GC, respectively. CD44 positivity significantly correlated with poor prognosis both in intestinal- and diffuse-type GC cases (intestinal-type: $P < 0.001$, diffuse-type: $P = 0.01$, log-rank test). CD133 positivity significantly correlated with poor prognosis in intestinal-type GC cases ($P = 0.004$, log-rank test). ALDH1 positivity had no prognostic impact in both histologic types (intestinal-type: $P = 0.93$, diffuse-type: $P = 0.91$, log-rank test).

To evaluate the potential for CSC markers as a prognostic classifier, the association of CSC markers expression with cancer-specific mortality was evaluated with both univariate and multivariate Cox proportional hazards analyses (Table 2). By univariate analysis, the TNM stage (HR, 6.37; 95% CI, 2.38–16.67; $P = 0.002$), CD44 expression (HR, 4.20; 95% CI, 1.92–9.09; $P < 0.001$), and CD133 expression (HR, 4.67; 95% CI, 1.08–20.00; $P = 0.04$) were associated with survival. By multivariate modeling, both CD44 expression (HR, 2.77; 95% CI, 1.19–6.25; $P = 0.02$) and CD133 expression (HR, 20.41; 95% CI, 3.70–100.00; $P < 0.001$) were independent prognostic indicators (Table 2). These results indicate that immunohistochemical examination of CD44 and CD133 in GC samples have potential as prognostic biomarkers for GC.

Comparison of CSC marker expression between primary and lymph node metastatic sites

Immunostaining of lymph node metastatic sites was performed. Compared with the positive rate and staining pattern of CSC markers in primary tumors, concordance rates were calculated as a combination of both positive and negative cases in primary and metastasis, divided by the total number of cases. Concordance rates of all CSC markers were more than 70% (Table 3). CSC markers expression pattern in lymph node metastasis tended to be the same as primary tumor (Fig. 3). Interestingly, when tumors were classified as intestinal-, diffuse- and mixed-types based on their Lauren classification, the positivity of ALDH1 in lymph node metastasis of the diffuse-type was significantly higher than that of the primary tumor ($P < 0.001$, χ^2 test, Table 4).

DISCUSSION

According to the CSC hypothesis, it is assumed that CSCs are responsible for cancer initiation and development. Expression of CSC markers have been reported to be present in normal adult stem/ progenitor cells as well as in CSC.[30,31] In this present study, we examined the expression and distribution of representative CSC markers (ALDH1, CD44 and CD133) in normal, metaplastic, and cancerous tissue of the stomach. Although we could not detect CSC marker staining in gastric pit, positive staining of CD44 and ALDH1 was detected at the crypt bottom of intestinal metaplasias, whose staining patterns closely resembled those of

Table 2 Univariate and multivariate Cox regression analysis of cancer stem cell (CSC) marker expression levels and overall survival (stage I-IV, $n = 65$)

Characteristic	Univariate analysis HR (95% CI)	*P*-value*	Multivariate analysis HR (95% CI)	*P*-value*
Age				
< 65	1 (Ref.)	0.41		
65 and 65<	1.38 (0.65–2.94)			
Sex				
Male	1 (Ref.)	0.40		
Female	0.72 (0.33–1.57)			
TNM stage†				
Stage I/II	1 (Ref.)	0.002	1 (Ref.)	0.002
Stage III/IV	6.37 (2.38–16.67)		6.41 (2.04–20.00)	
ALDH1 expression				
Negative	1 (Ref.)	0.40		
Positive	1.41 (0.32–1.57)			
Histology				
Intestinal	1	0.38		
Diffuse and mixed	1.27 (0.56–2.43)			
Histology				
Intestinal and mixed	1	0.21		
Diffuse	0.86 (0.24–1.22)			
CD44 expression				
Negative	1 (Ref.)	<0.001	1 (Ref.)	0.02
Positive	4.20 (1.92–9.09)		2.77 (1.19–6.25)	
CD133 expression				
Negative	1 (Ref.)	0.04	1 (Ref.)	<0.001
Positive	4.67 (1.09–20.00)		20.41 (3.70–100.00)	

*χ^2 test: $P < 0.05$ was considered significant.

†Tumor stage was classified according to the criteria of the International Union Against Cancer Tumor Node Metastasis (TNM) classification of malignant tumors.

ALDH1, aldehyde dehydrogenase 1; CI, confidence interval; HR, hazard ratio.

Table 3 Positive rate and concordance rate of cancer stem cell (CSC) marker expression in primary gastric cancer (GC) and metastasis

Total	Positive rate	Concordance rate†
ALDH1		
Primary	60/104 (57%)	73/104 (70%)
Metastasis	77/104 (74%)	
CD44		
Primary	60/104 (57%)	78/104 (75%)
Metastasis	62/104 (59%)	
CD133		
Primary	14/104 (13%)	91/104 (87%)
Metastasis	9/104 (8%)	

†Concordance rate; calculated as a combination of both positive and negative cases in primary and metastasis, divided by total number of cases.

ALDH1, aldehyde dehydrogenase 1.

the normal colon.[20,26] Taken together, immunohistochemical analysis of these markers are not useful for detecting normal stem cells of the stomach. In GC, we found 55% and 62% were positive for ALDH1 and CD44, respectively, and stained cancer cells of these markers were frequently observed in a wide sphere of tumor lesions. Compared with these markers, only 9% were CD133-positive cases, and CD133-positive cancer cells were observed less-frequently (10–40%) and in a narrower range of lesions. It has been reported that CSCs occupies less than a few percent of whole number of cancer cells.[2,20,32] Therefore, it could be speculated that all markers examined in this present study labeled a larger cell population with some stem cell-like characteristics. Although these markers have been used to identify and isolate both normal and malignant stem cells in many human organs, the specificity for detecting stem cells remains uncertain. Further work to clarify the CSC-like properties of these subpopulations in GC will aid GC stem cell research.

It is also presumed that CSCs can disseminate from the primary tumor to distant sites.[33] In this study, we examined the expression and distribution of CSC markers in both primary and lymph node metastatic sites of GC, and studied the relationship between CSC marker staining and clinicopathologic characteristics. Although few epithelial cells in non-neoplastic gastric mucosa showed CD44 and CD133 staining and only parietal cells were labeled by ALDH1, strong and extensive staining of CSC markers was found in many GC cases. Moreover, CSC markers-positive cases had significant correlations with advanced T grade, N grade or

Table 4 Association between cancer stem cell (CSC) marker expression and morphology in primary gastric cancer (GC) and metastasis

Intestinal-type	Positive rate	*P*-value*
ALDH1		
Primary	31/37 (85%)	0.13
Metastasis	34/46 (74%)	
CD44		
Primary	22/37 (60%)	0.84
Metastasis	28/46 (62%)	
CD133		
Primary	8/37 (21%)	0.28
Metastasis	6/46 (14%)	
Diffuse-type		*P*-value*
ALDH1		
Primary	23/54 (43%)	<0.001
Metastasis	39/47 (83%)	
CD44		
Primary	30/54 (56%)	0.84
Metastasis	28/47 (60%)	
CD133		
Primary	5/54 (9%)	0.79
Metastasis	3/47 (6%)	
Mixed-type		*P*-value*
ALDH1		
Primary	6/13 (46%)	0.70
Metastasis	4/11 (36%)	
CD44		
Primary	8/13 (61%)	1.00
Metastasis	6/11 (54%)	
CD133		
Primary	1/13 (7%)	–
Metastasis	0/11 (0%)	

*χ^2 test: $P < 0.05$ was considered significant.
ALDH1, aldehyde dehydrogenase 1.

stage. On the other hand, staining with CD44 and CD133 had significant prognostic impact in all analysis conditions (all stages, more than stage II, only stage II and III), and multivariate analysis revealed that CD44 and CD133 expression were independent prognostic factors. Based on these results, worse values OS in CD44- and CD133-positive cases were considered not to be simply because these positive cases contained more advance stages. These results are consistent with previous reports that CSC marker expression is significantly upregulated in some solid carcinomas and are risk factors for worse clinical behavior.[25,26,34] Of three CSC markers, CD44 is well known as a target gene of non-canonical WNT signaling cascade and has been implicated in a wide variety of pathological processes and cancer cell biology, such as invasion metastasis.[35,36] However, with regard to CD133 and ALDH1, details of associated functions involving not only CSCs but also normal cells are unclear. In this present study, we found that the positivity of ALDH1 in diffuse-type lymph node metastasis was significantly higher than that of the primary tumor. In diffuse-type GC, it has been reported that transforming growth factor-β (TGF-β) signaling directly represses the transcription of ABCG2, which was used to identify SP cells and negatively contributes to the maintenance of CSCs within the cancer.[37] However, it is well-known that ABCG2 is not directly involved in the tumor-forming ability of SP cells.[38] A correlation between TGF-β signaling and CSC remains obscure. Some recent studies have shown that combination analyses of multiple CSC markers can further restrict the phenotypic definition of CSCs and isolate an even more tumorigenic subset.[17,19] To shed light on the function of ALDH1 and CD133 in cancer tissue, it is necessary to investigate mutual interactions of these CSC marker molecules and study whether CD133 and ALDH1 are involved in WNT or TGF-β signaling, which would help to identify cells of multiple CSC phenotypes.

In summary, we demonstrated the staining properties of CSC markers in normal, metaplastic and cancerous tissue of the stomach. The CSC markers were associated with tumor progression. Both CD44 and CD133 are independent markers for poor survival in patients with GC. However, the detailed functions of CD133 and ALDH1 in GC remain unclear. Clarification of the correlation among these CSC markers may lead to the identification of essential CSC features.

ACKNOWLEDGMENTS

We thank Mr Shinichi Norimura for excellent technical assistance and advice. We also thank the Analysis Center of Life Science, Hiroshima University, for the use of their facilities. This work was supported in part by Grants-in-Aid for Cancer Research from the Ministry of Education, Culture, Science, Sports, and Technology of Japan; in part by Grants-in-Aid for the Third Comprehensive 10-Year Strategy for Cancer Control and for Cancer Research from the Ministry of Health, Labour and Welfare of Japan.

REFERENCES

1 Ohgaki H, Matsukura N. Stomach cancer. In: Stewart BW, Kleihues P, eds. *World Cancer Report*. Lyon: IARC Press, 2003; 197.
2 Reya T, Morrison SJ, Clarke MF, Weissman IL. Stem cells, cancer, and cancer stem cells. *Nature* 2001; **414**: 105–11.
3 Clark MF, Fuller M. Stem cells and cancer: Two faces of eve. *Cell* 2006; **124**: 1111–15.
4 Visvader JE, Lindeman GJ. Cancer stem cells in solid tumours: Accumulating evidence and unresolved questions. *Nat Rev Cancer* 2008; **8**: 755–68.
5 Singh SK, Hawkins C, Clarke ID *et al.* Identification of human brain tumour initiating cells. *Nature* 2004; **432**: 396–401.
6 Ricci-Vitiani L, Lombardi DG, Pilozzi E *et al.* Identification and expansion of human colon-cancer-initiating cells. *Nature* 2007; **445**: 111–5.

7 Singh SK, Clarke ID, Terasaki M *et al.* Identification of a cancer stem cell in human brain tumors. *Cancer Res* 2003; **63**: 5821–8.
8 Ishigami S, Ueno S, Arigami T *et al.* Prognostic impact of CD133 expression in gastric carcinoma. *Anticancer Res* 2010; **30**: 2453–7.
9 Zhao P, Li Y, Lu Y. Aberrant expression of CD133 protein correlates with Ki-67 expression and is a prognostic marker in gastric adenocarcinoma. *BMC Cancer* 2010; **10**: 218–23.
10 Nagano O, Murakami D, Hartmann D *et al.* Cell-matrix interaction via CD44 is independently regulated by different metalloproteinases activated in response to extracellular Ca(2+) influx and PKC activation. *J Cell Biol* 2004; **165**: 893–902.
11 Vigetti D, Viola M, Karousou E *et al.* Hyaluronan-CD44-ERK1/2 regulate human aortic smooth muscle cell motility during aging. *J Biol Chem* 2008; **283**: 4448–58.
12 Aruffo A, Stamenkovic I, Melnick M, Underhill CB, Seed B. CD44 is the principal cell surface receptor for hyaluronate. *Cell* 1990; **61**: 1303–13.
13 Al-Hajj M, Wicha MS, Benito-Hernandez A, Morrison SJ, Clarke MF. Prospective identification of tumorigenic breast cancer cells. *Proc Natl Acad Sci U S A* 2003; **100**: 3983–8.
14 Yasui W, Kudo Y, Naka K *et al.* Expression of CD44 containing variant exon 9 (CD44v9) in gastric adenomas and adenocarcinomas: Relation to the proliferation and progression. *Int J Oncol* 1998; **12**: 1253–8.
15 Collins AT, Berry PA, Hyde C, Stower MJ, Maitland NJ. Prospective identification of tumorigenic prostate cancer stem cells. *Cancer Res* 2005; **65**: 10946–51.
16 Li C, Heidt DG, Dalerba P *et al.* Identification of pancreatic cancer stem cells. *Cancer Res* 2007; **67**: 1030–7.
17 Dalerba P, Dylla SJ, Park IK *et al.* Phenotypic characterization of human colorectal cancer stem cells. *Proc Natl Acad Sci U S A* 2007; **104**: 10158–63.
18 Takaishi S, Okumura T, Tu S *et al.* Identification of gastric cancer stem cells using the cell surface marker CD44. *Stem Cells* 2009; **27**: 1006–20.
19 Ginestier C, Hur MH, Charafe-Jauffret E *et al.* ALDH1 is a marker of normal and malignant human mammary stem cells and a predictor of poor clinical outcome. *Cell Stem Cell* 2007; **1**: 555–67.
20 Huang EH, Hynes MJ, Zhang T *et al.* Aldehyde dehydrogenase 1 is a marker for normal and malignant human colonic stem cells (SC) and tracks SC overpopulation during colon tumorigenesis. *Cancer Res* 2009; **69**: 3382–9.
21 Moreb J, Schweder M, Suresh A, Zucali JR. Overexpression of the human aldehyde dehydrogenase class I results in increased resistance to 4-hydroperoxycyclophosphamide. *Cancer Gene Ther* 1996; **3**: 24–30.
22 Liang D, Shi Y. Aldehyde dehydrogenase-1 is a specific marker for stem cells in human lung adenocarcinoma. *Med Oncol* (in press).
23 Jiang F, Qiu Q, Khanna A *et al.* Aldehyde dehydrogenase 1 is a tumor stem cell-associated marker in lung cancer. *Mol Cancer Res* 2009; **7**: 330–8.
24 Oue N, Mitani Y, Aung PP *et al.* Expression and localization of Reg IV in human neoplastic and non-neoplastic tissues: Reg IV expression is associated with intestinal and neuroendocrine differentiation in gastric adenocarcinoma. *J Pathol* 2005; **207**: 185–98.
25 Kojima M, Ishii G, Atsumi N *et al.* Immunohistochemical detection of CD133 expression in colorectal cancer: A clinicopathological study. *Cancer Sci* 2008; **99**: 1578–83.
26 Shimada Y, Ishii G, Nagai K *et al.* Expression of podoplanin, CD44, and p63 in squamous cell carcinoma of the lung. *Cancer Sci* 2009; **100**: 2054–9.
27 Jiang F, Qiu Q, Khanna A *et al.* Aldehyde dehydrogenase 1 is a tumor stem cell-associated marker in lung cancer. *Mol Cancer Res* 2009; **7**: 330–8.
28 Harn HJ, Ho LI, Chang JY *et al.* Differential expression of the human metastasis adhesion molecule CD44V in normal and carcinomatous stomach mucosa of Chinese subjects. *Cancer* 1995; **75**: 1065–71.
29 Du L, Wang H, He L *et al.* CD44 is of functional importance for colorectal cancer stem cells. *Clin Cancer Res* 2008; **14**: 6751–60.
30 Clevers H. The cancer stem cell: Premises, promises and challenges. *Nat Med* 2011; **17**: 313–9.
31 Mills JC, Shivdasani RA. Gastric epithelial stem cells. *Gastroenterology* 2011; **140**: 412–24.
32 Lee CJ, Li C, Simeone DM. Human pancreatic cancer stem cells: Implications for how we treat pancreatic cancer. *Transl Oncol* 2008; **1**: 14–8.
33 Pantel K, Alix-Panabières C, Riethdorf S. Cancer micrometastases. *Nat Rev Clin Oncol* 2009; **6**: 339–51.
34 Charafe-Jauffret E, Ginestier C, Iovino F *et al.* Aldehyde dehydrogenase 1-positive cancer stem cells mediate metastasis and poor clinical outcome in inflammatory breast cancer. *Clin Cancer Res* 2010; **16**: 45–55.
35 Ponta H, Sherman L, Herrlich A. CD44: From adhesion molecules to signalling regulators. *Nat Rev Mol Cell Biol* 2003; **4**: 33–45.
36 Ishimoto T, Oshima H, Oshima M *et al.* CD44+ slow-cycling tumor cell expansion is triggered by cooperative actions of Wnt and prostaglandin E2 in gastric tumorigenesis. *Cancer Sci* 2010; **101**: 673–8.
37 Ehata S, Johansson E, Katayama R *et al.* Transforming growth factor-β decreases the cancer-initiating cell population within diffuse-type gastric carcinoma cells. *Oncogene* 2011; **30**: 1693–705.
38 Patrawala L, Calhoun T, Schneider-Broussard R, Zhou J, Claypool K, Tang DG. Side population is enriched in tumorigenic, stem-like cancer cells, whereas ABCG2+ and ABCG2- cancer cells are similarly tumorigenic. *Cancer Res* 2005; **65**: 6207–19.

GASTROENTEROLOGY 2012;142:292-304

Deficiency of Claudin-18 Causes Paracellular H^+ Leakage, Up-regulation of Interleukin-1β, and Atrophic Gastritis in Mice

DAISUKE HAYASHI,*,‡ ATSUSHI TAMURA,* HIROO TANAKA,* YUJI YAMAZAKI,* SHIN WATANABE,* KOYA SUZUKI,* KAZUO SUZUKI,§ KAZUHIRO SENTANI,‖ WATARU YASUI,‖ HIROMI RAKUGI,‡ YOSHITAKA ISAKA,‡ and SACHIKO TSUKITA*

*Laboratory of Biological Science, Graduate School of Frontier Biosciences and Graduate School of Medicine, and ‡Department of Geriatric Medicine and Nephrology, Graduate School of Medicine, Osaka University, Osaka; §Department of Immunology, Graduate School of Medicine, Chiba University, Chiba; and ‖Department of Molecular Pathology, Hiroshima University Graduate School of Biomedical Sciences, Hiroshima, Japan

See the Covering the Cover synopsis on page 192.

BACKGROUND & AIMS: Although defects in tight junction (TJ) epithelial paracellular barrier function are believed to be a primary cause of inflammation, the mechanisms responsible remain largely unknown. **METHODS:** We generated knockout mice of stomach-type claudin-18, a major component of TJs in the stomach. **RESULTS:** *Cldn18*$^{-/-}$ mice were afflicted with atrophic gastritis that started on postnatal day 3. This coincided with a decrease in intragastric pH due to H^+ secretion from parietal cells and concomitant up-regulation of the cytokines, interleukin-1β, cyclooxygenase-2, and KC, resulting in spasmolytic polypeptide-expressing metaplasia (SPEM). Oral administration of hydrochloric acid on postnatal day 1 induced the expression of these cytokines in *Cldn18*$^{-/-}$ infant stomach, but not in *Cldn18*$^{+/+}$ mice. A paracellular H^+ leak in *Cldn18*$^{-/-}$ stomach was detected by electrophysiology and H^+ titration, and freeze-fracture electron microscopy showed structural defects in the TJs, in which the tightly packed claudin-18 (stomach-type)-based TJ strands were lost, leaving a loose meshwork of strands consisting of other claudin species. **CONCLUSIONS: These findings provide evidence that claudin-18 normally forms a paracellular barrier against H^+ in the stomach and that its deficiency causes paracellular H^+ leak, a persistent up-regulation of proinflammatory cytokines, chronic recruitment of neutrophils, and the subsequent development of SPEM in atrophic gastritis.**

Keywords: Claudin; Gene Knockout; Tight Junction; Gastritis.

BASIC AND TRANSLATIONAL AT

The epithelial system defines the parameters of biological homeostasis in multicellular organisms, including the immunologic defense system.[1,2] Epithelial cells adhere to each other to form cell sheets, and when the intercellular spaces between epithelial cells are sealed by tight junctions (TJs), the paracellular barrier function is established.[3-7] The gastric epithelia are specifically resistant to hazardous materials, such as strong acids and the protease pepsin.[8] Defects in these security systems are assumed to cause diseases such as gastritis.[8-10] Chronic gastritis is a risk factor for gastric cancer, and a major cause of gastritis is infection by *Helicobacter pylori*.[11-14] Specific inflammation-related interleukins (ILs), tumor necrosis factor (TNF)-α, interferons, and prostaglandins are reportedly involved in the recruitment of inflammatory cells to chronically inflamed tissue.[15,16] On the other hand, the cell-cell adhesion system that typifies epithelial cell sheets may be important in establishing a bulwark against gastric inflammation.[17-19]

In epithelial cell sheets, the TJ system is primarily responsible for establishing the paracellular barrier function.[20,21] The TJ is a supramolecular complex in which combinations of several kinds of transmembrane proteins, including claudins, TAMPs, and JAMs, are associated with membrane-scaffolding proteins such as ZO-1/2 and cingulin,[22-24] allowing the dynamic regulation of ion and solute passage across the paracellular space. Among the TJ proteins, claudins are specifically required to form the TJ strands that organize the paracellular barrier structure.[3,4,25,26] The multi-gene claudin family has at least 27 members in human/mouse.[3,27] Although claudins are paracellular barrier-forming proteins, there do exist "ion-leaky" claudins that allow specific ions to cross the barrier.[26,28-30] One of the most remarkable characteristics of claudin family proteins is their distinct, tissue function-dependent expression patterns.[27,31]

Claudin-18 has two alternative splicing forms, the lung and stomach types, which use a different first exon and the same exons 2-4; the two isoforms are regulated by different tissue-specific promotors.[32] Because the stomach-type claudin-18 is the predominant claudin expressed in stomach, it is expected to regulate the stomach-specific properties of the paracellular barrier, including resistance to H^+ leakage and/or pepsin, as implied by its overexpression in MDCK II cells.[19] In this study, to understand the role of stomach-type claudin-18 in gastric epithelia, we generated and analyzed knockout mice of stomach-type claudin-18 (*Cldn18*$^{-/-}$ mice).

Abbreviations used in this paper: COX, cyclooxygenase; IF, intrinsic factor; IL, interleukin; qRT-PCR, quantitative real-time polymerase chain reaction; SPEM, spasmolytic polypeptide-expressing metaplasia; TJ, tight junction; TNF, tumor necrosis factor.

0016-5085/$36.00
doi:10.1053/j.gastro.2011.10.040

Using electrophysiologic, H^+-titrational measurements, and electron microscopic analyses, we found that the TJ-mediated barrier against H^+ leakage was impaired in *Cldn18*$^{-/-}$ stomach. Infant *Cldn18*$^{-/-}$ mice developed atrophic gastritis once the intragastric pH began to decrease. This gastritis involved the up-regulation of IL-1β and a consistent infiltration of neutrophils. Our findings strongly suggest that H^+ leakage across the gastric epithelia was the major cause of gastritis in the *Cldn18*$^{-/-}$ mice. These findings may provide a new paradigm for understanding the regulation of chronic inflammation in general.

Materials and Methods

Generation of Cldn18$^{-/-}$ *Mice and Histology*

The targeting vector was constructed as shown (Figure 1). Animal experiments were performed as previously described.[30,33-35]

Antibodies

The primary antibodies for intrinsic factor (IF) was generously provided by Drs J. Mills and D. Alpers[36,37] and for E-cadherin antibody was generously provided by Dr M. Takeichi. All other antibodies used are described in Supplementary Materials and Methods.

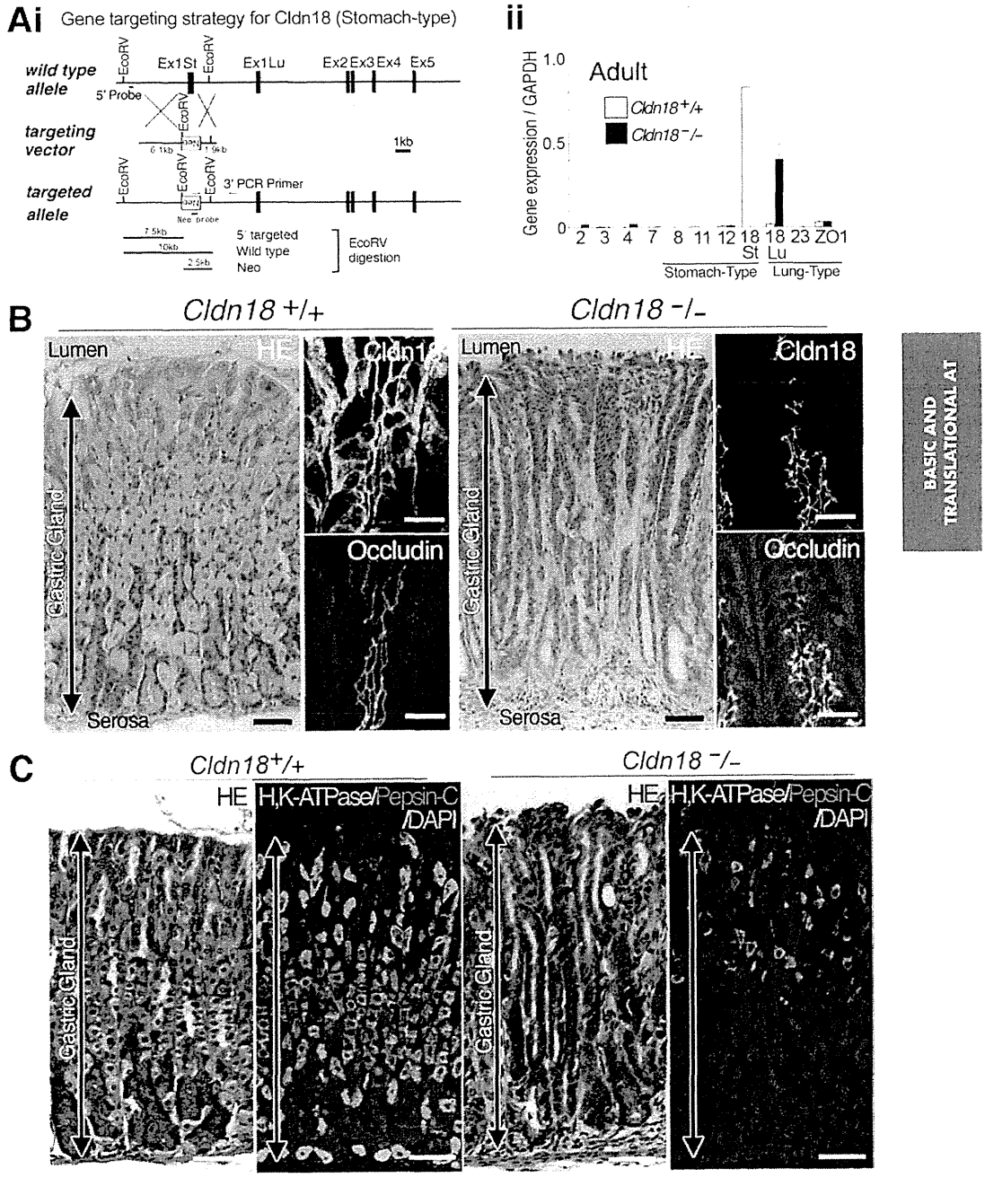

Figure 1. Generation of stomach-type claudin-18 knockout mice. (*A* [*i*]) Construction of the wild-type allele, targeting vector, and targeted allele of the mouse claudin-18 gene. (*A* [*ii*]) Gene expression of claudin family members in *Cldn18*$^{+/+}$ and *Cldn18*$^{-/-}$ adult stomach, as determined by qRT-PCR ($n \geqq 4$). (*B*) Light microscopic images of H&E-stained paraffin sections and immunofluorescence of frozen sections of *Cldn18*$^{+/+}$ and *Cldn18*$^{-/-}$ stomach for claudin-18 and occludin. *Bars* = 50 μm (color panels) and 20 μm (gray panels). (*C*) Light microscopic images of H&E-stained paraffin sections and immunofluorescence images of sections stained with antibodies against H^+,K^+-ATPase (H,K-ATPase) and pepsin C. *Bars* = 50 μm.

Electrophysiology and Proton, Biotin, and Dextran Permeation Assays

The conductance, dilution potential, and permeability of H^+ and dextran were measured using an Ussing 2-chamber apparatus.[19,30,38] Biotin permeation was measured by previously described methods.[33]

Gene Expression Assays and Measurement of Cytokine Levels by Enzyme-Linked Immunosorbent Assay

Quantitative real-time polymerase chain reaction (qRT-PCR) was performed as described previously (Supplementary Table 1).[33] The levels of IL-1β and IL-6 in *Cldn18*$^{+/+}$ and *Cldn18*$^{-/-}$ mouse serum were determined using an enzyme-linked immunosorbent assay kit (BD Biosciences, NJ).

Single Cell Preparation and Fluorescence-Activated Cell Sorter Analysis

Stomach samples were processed as previously described but with slight modifications.[39]

Ultrathin-Section Electron Microscopy and Freeze-Fracture Replica Electron Microscopy

Samples were processed as previously described in the Supplementary Materials and Methods Section.[33]

Statistical Analysis

Results are expressed as means ± SEM. P values were calculated using an independent t test, with $P < .05$ considered significant.

See Supplementary Materials and Methods for more details.

Results

Generation of Stomach-Type Claudin-18 Knockout Mice

Two splicing forms of claudin-18, stomach-type variant 2 and lung-type variant 1, are the respective predominant claudins in mouse stomach and lung (Figure 1*A* and Supplementary Figure 1). In adult stomach, there were low levels of all the claudins except claudin-18, including claudin-2, -3, -4, -7, -8, -11, -12, and -23, as shown by quantitative assessment of their messenger RNAs (Figure 1*A*). Here, we generated stomach-type *Cldn18* knockout (*Cldn18*$^{-/-}$) mice, which had no obvious macroscopic abnormalities throughout their life span (data not shown).

In adult *Cldn18*$^{-/-}$ stomach, although lung-type claudin-18 was up-regulated, as shown by qRT-PCR (Figure 1*A* and Supplementary Figure 1), the presence of gastritis indicates that this did not compensate for the loss of stomach-type claudin-18. The staining distributions of the two types of claudin-18 was different; the stomach type was expressed in the TJ/lateral membrane and the lung type in the TJs (see Figure 1*B* and Supplementary Figure 2). Furthermore, there was a slight difference in the distribution and expression level of claudin-2 between *Cldn18*$^{+/+}$ and *Cldn18*$^{-/-}$ stomach in adults (Supplementary Figure 2), similar messenger RNA and protein expression levels of occludin in both infant and adult Cldn18$^{+/+}$ and Cldn18$^{-/-}$ stomach, and a slight decrease in the tight junctional localization of Cldn18$^{-/-}$ adult superficial mucous epithelial cells (Supplementary Figure 3). No obvious changes in the levels of other cell-cell adhesion-related proteins were found between the *Cldn18*$^{+/+}$ and *Cldn18*$^{-/-}$ stomach (Supplementary Figure 2*A*).

Characterization of Gastritis in Stomach-Type Claudin-18 Knockout Mice

Tissue-level examination revealed chronic gastritis in adult *Cldn18*$^{-/-}$ stomach (Figure 1*B* and *C* and Supplementary Figure 4). In H&E-stained preparations, the gastric gland of adult *Cldn18*$^{+/+}$ mice showed typical cell type distribution, with parietal cells predominant at the midlevel region and chief cells predominant at the basal region. In contrast, in *Cldn18*$^{-/-}$ stomach, there were far fewer parietal and chief cells, which had largely been replaced by metaplastic cells with dilated gland lumina (Figure 1*B* and *C* and Supplementary Figures 4 and 5). Furthermore, inflammatory cells were abundant in the *Cldn18*$^{-/-}$ submucosal region. Finally, the incidence of gastritis was 100% in *Cldn18*$^{-/-}$ mice.

Close examination of H&E-stained samples and sections immunostained with specific markers for parietal (anti-H^+,K^+-adenosine triphosphatase [ATPase]) and chief cells (anti-pepsin C/anti-IF) showed that their numbers, as well as that of mature surface mucous cells, were lower than normal in the *Cldn18*$^{-/-}$ gastric mucosa, which was consistent with the difference we observed in the position of the Ki-67-positive proliferative zone (Supplementary Figure 6). These findings were confirmed by qRT-PCR experiments that showed down-regulation of H^+,K^+-ATPase, IF, and MUC5AC (Supplementary Figure 7).

Down-regulation of Claudin-18 Expression in Human Gastric Metaplasia

Because previous studies reported the down-regulation of claudin-18 expression in human gastric cancer,[40] we investigated the expression levels of claudin-18 in human chronic and autoimmune gastritis by an immunohistochemical survey. We found that claudin-18 was down-regulated in human gastritis specimens at foci that showed atrophy and metaplasia. In superficial gastritis, the claudin-18 level was also decreased. Thus, claudin-18 is probably down-regulated pathologically in human gastritic tissue (Figure 2 and Supplementary Figure 8), suggesting that mouse *Cldn18*$^{-/-}$ gastritis may be a good model system for human disease.

Changes in the TJ Strands of Claudin-18–Deficient Mice

Because claudin-18 is the major TJ component of stomach epithelial cells, we examined TJ morphology by electron microscopy (Figure 3). In *Cldn18*$^{+/+}$ stomach at low magnification, well-differentiated parietal cells and chief cells around the lumen of the gland were visible. In contrast, spasmolytic polypeptide-expressing metaplasia (SPEM) cells were dominant in *Cldn*18$^{-/-}$ stomach, with few number of

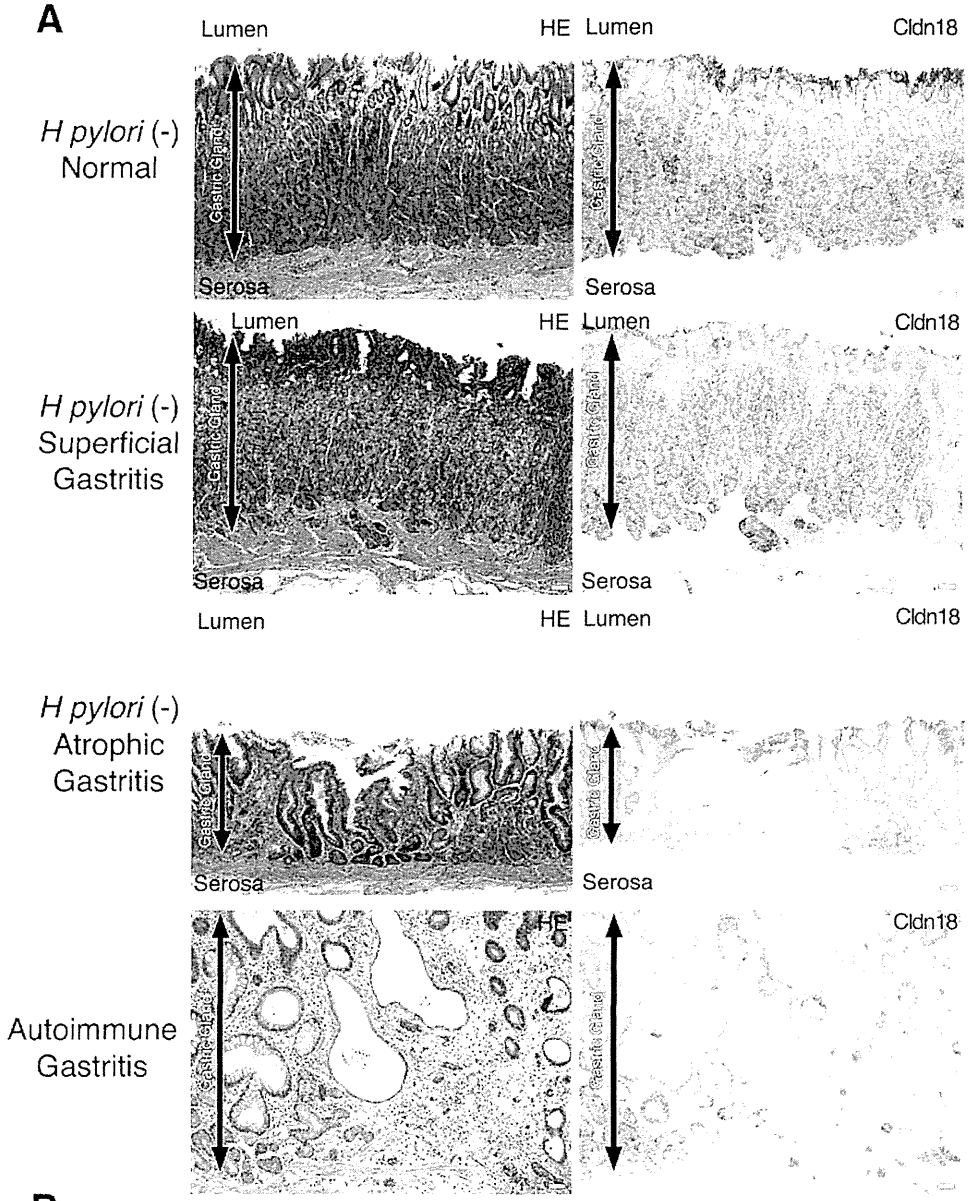

B

Expression of Cldn18 (0 ~ 4+)	4+	3+	2+	1+	0
Normal (n=9)	9 (100%)	0	0	0	0
Chronic superficial gastritis (n=28)	19 (68%)	8 (29%)	1 (4%)	0	0
Chronic atrophic gastritis (n=37)	3 (8%)	6 (16%)	15 (41%)	12 (32%)	1 (3%)
Intestinal metaplasia (n=41)	0	0	2 (5%)	22 (54%)	17 (41%)

Expression of Cldn18

4+ ; 75-100%
3+ ; 50-75%
2+ ; 25-50%
1+ ; 1-25%
0 ; 0%

Figure 2. Human gastritis studies show a down-regulation of stomach-type claudin-18. (*A*) H&E-stained and immunohistochemically claudin-18–stained micrographs of paraffin sections from normal and gastritic regions of a human stomach. Claudin-18 is down-regulated in gastritis. (*B*) Statistical information about the expression of claudin-18 in human gastritis. *Bars* = 50 μm.

well-differentiated parietal and chief cells (Figure 3*A*). Additionally, high magnification showed noticeably reduced TJ width in *Cldn18*$^{-/-}$ stomach (Figure 3*B*).

For TJs to exert their barrier function, TJ strands must be formed. In some tissues, the morphology of the TJ strands at least partly reflects the ability of TJs to function. Freeze-fracture electron microscopy showed highly H^+-resistant TJ strands in adult *Cldn18*$^{+/+}$ stomach as double layers. The most apical layer consisted of tightly packed parallel TJ strands, below which was a layer of much more loosely anastomosing strands (Figure 3*C*). In *Cldn18*$^{-/-}$ stomach, the upper layer of the TJ strands was missing, which explained the decreased TJ width in thin-section electron micrographs of *Cldn18*$^{-/-}$ stomach. Considering the predominant expression of claudin-18 in *Cldn18*$^{+/+}$ stomach, the upper layer of tightly packed TJ strands probably consists largely of stomach-type claudin-18 and forms a highly H^+-resistant paracellular bar-

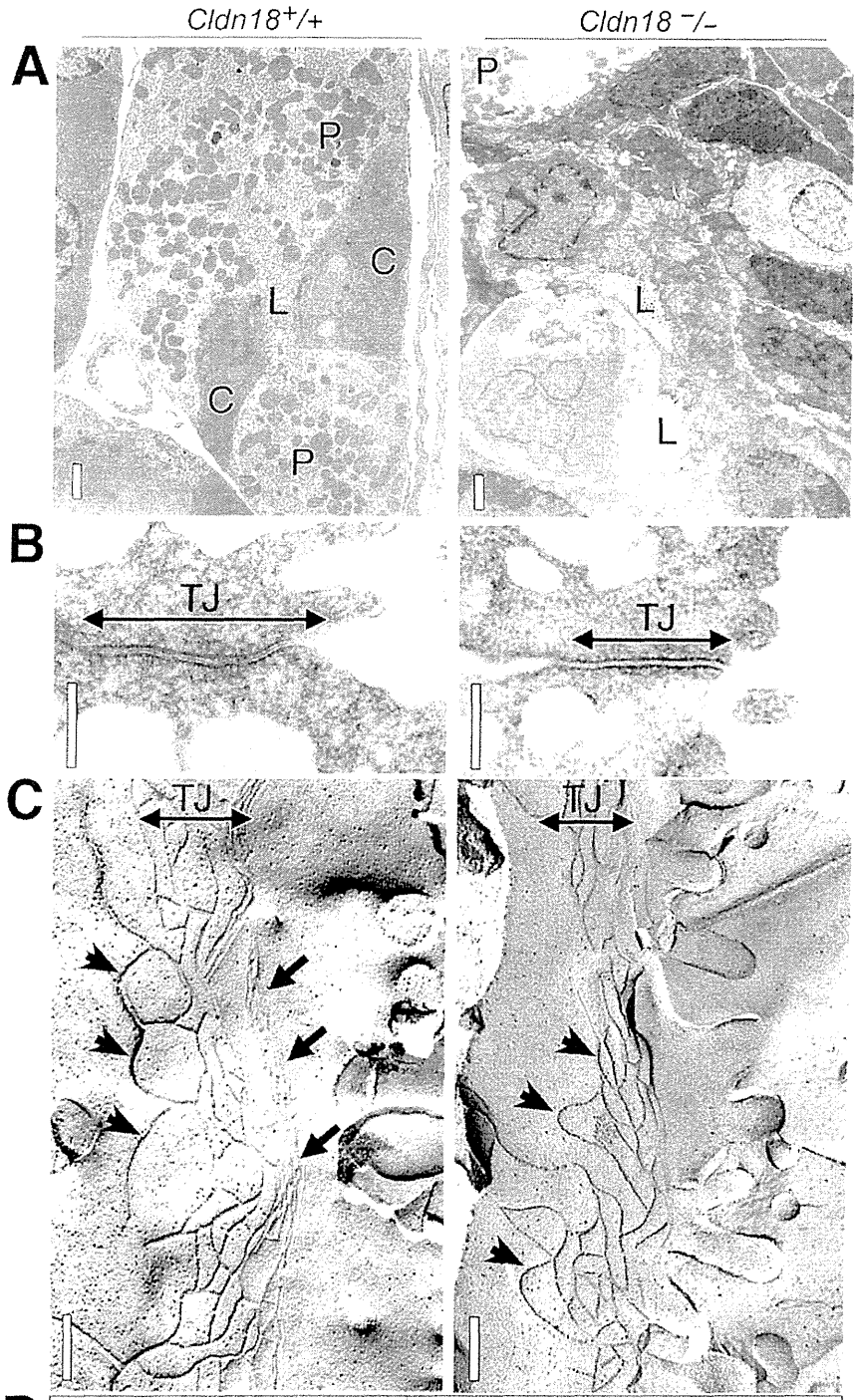

D

		Number of strands*	Interval of strands (nm)*
Packed superior region	Cldn18+/+	3.27±0.23	0.73±0.03
	Cldn18−/−	0.30±0.14	1.12±0.01
		(*P*<<.01)	(*P*=.009)
Non packed inferior region	Cldn18+/+	4.60±0.17	4.08±0.22
	Cldn18−/−	4.89±0.30	4.27±0.30
		(*P*=.41)	(*P*=.62)

*Intervals and Number of strands on a line drawn perpendicular to the junctional axis. Mean ± SEM.

Figure 3. Electron microscopic characterization of *Cldn18*$^{+/+}$ and *Cldn18*$^{-/-}$ stomach. (*A* and *B*) Thin-section electron microscopic images of TJs in *Cldn18*$^{+/+}$ and *Cldn18*$^{-/-}$ stomach. L, lumen of gastric glands; P, parietal cells; C, chief cells. *Bars* = 1 μm. (*C*) Freeze-fracture electron microscopic images of TJ strands in *Cldn18*$^{+/+}$ and *Cldn18*$^{-/-}$ stomach. Densely packed TJ strands (*arrows*) in the apical region of *Cldn18*$^{+/+}$ gastric epithelial cells were absent in the *Cldn18*$^{-/-}$ cells, which instead showed loosely anastomosing TJ strands (*arrowheads*). *Bars* = 1 μm. (*D*) Statistical information about the numbers and densities of TJ strands in *Cldn18*$^{+/+}$ and *Cldn18*$^{-/-}$ gastric epithelial cells.

rier. The quantification[33] of TJ strands allowed us to estimate an average number of strands to which stomach-type claudin-18 contributes to be approximately 3.0. On the other hand, the lower layer of loosely anastomosing TJ strands may consist of various types of claudins (Figure 3*D*). Together, these results suggest that stomach-type claudin-18 is important for morphologically distinct, parallel, tightly packed TJ strands and that TJ strands in the stomach may functionally specialize to create a paracellular barrier against H^+.

Characterization of Gastritis in Cldn18$^{-/-}$ Stomach by Histologic Examination and by Inflammation-Related Biomarkers

The gastric epithelium of *Cldn18*$^{-/-}$ stomach was largely occupied by proliferating mucous-like cells positive for TFF2 (Figure 4*A* and Supplementary Figure 7). Some of these cells were also positive for IF, indicating SPEM[9] (Figure 4). Thus, adult *Cldn18*$^{-/-}$ mouse stomach showed characteristics of atrophic gastritis, an interpretation supported by the down-regulation of genes for H^+,K^+-ATPase and IF and up-regulation of the TFF2 gene, as assessed by qRT-PCR (Supplementary Figure 7). Finally, HE4,[41] another marker for metaplasia, was also up-regulated, although no cancerous changes were detected histologically (Supplementary Figure 9).

Claudin-18 Deficiency Induced Changes in Inflammation Markers in Cldn18$^{-/-}$ Stomach

Next, to characterize the inflammation induced by claudin-18 deficiency, the expressions of various inflammation markers were examined in adult *Cldn18*$^{+/+}$ and *Cldn18*$^{-/-}$ stomachs. *Cldn18*$^{-/-}$ stomachs had higher expressions of the proinflammatory markers IL-1β and TNF-α (Figure 4*B*). We also found that the levels of the neutrophil chemoattractant KC were significantly higher in the *Cldn18*$^{-/-}$ stomach than the *Cldn18*$^{+/+}$ stomach, by qRT-PCR, with a slight up-regulation in MCP-1. In addition, consistent with the reported role of IL-1β in gastritis, we found that the protein level of serum IL-1β was up-regulated in *Cldn18*$^{-/-}$ mice (Figure 4*B*). Analysis of immune cell types by fluorescence-activated cell sorting revealed that neutrophils, which are positive for Gr-1 and negative for CD11b, predominated in gastritic *Cldn18*$^{-/-}$ tissue (Figure 4*C*). This is in agreement with our finding by immunofluorescence that neutrophils, but not macrophages, significantly increased in *Cldn18*$^{-/-}$ stomach of mice younger than 20 weeks of age (Figure 4*D* and Supplementary Figures 4 and 5).

The expression level of cyclooxygenase (COX)-2 was also higher in *Cldn18*$^{-/-}$ stomach, suggesting the involvement of prostaglandin E_2-related inflammation/restoration reactions (Figure 4*B*). There were no detectable changes in the expression levels of IL-2, IL-4, or IL-6 in the gastritic tissue, however, and no significant changes in the serum level of IL-6, suggesting that B cell and T cell-related immune systems were not significantly involved in this type of gastritis (Supplementary Figure 10).

The changes of tissue constitution associated with gastritis, as detected in *Cldn18*$^{-/-}$ corpus described previously, were not seen in *Cldn18*$^{-/-}$ antrum, consistently with that TFF2 expression was significantly changed in *Cldn18*$^{-/-}$ corpus but not in *Cldn18*$^{-/-}$ antrum. However, the increase in inflammation markers such as IL-1β was similarly induced for *Cldn18*$^{-/-}$ corpus and *Cldn18*$^{-/-}$ antrum. Possibly in this relation, gastrin expression was not up-regulated in the achlorhydric state of *Cldn18*$^{-/-}$ mice (Supplementary Figure 11*E*).

Age of Onset of Gastritis in Cldn18$^{-/-}$ Stomach

To discern the age of onset of gastritis, we first examined stomach specimens histologically. We did not find significant histologic differences between *Cldn18*$^{+/+}$ and *Cldn18*$^{-/-}$ stomachs at postnatal days 1–3 (Figure 5*A*). In postnatal day 4 mice, the number of H^+,K^+-ATPase-positive parietal cells in *Cldn18*$^{-/-}$ stomach showed a slight decrease compared with *Cldn18*$^{+/+}$ stomach. This difference in number became significant at postnatal day 7 (Figure 5*B*). Consistent with these results, qRT-PCR detected a decrease in the expression of H^+,K^+-ATPase and IF in *Cldn18*$^{-/-}$ stomachs (Figure 5*C*).

Acidification of the stomach lumen was detected at postnatal day 3 in *Cldn18*$^{+/+}$ stomach and increased at least until postnatal day 14 (Figure 6). In contrast, although some acidification was detected at postnatal day 3 in *Cldn18*$^{-/-}$ stomach, it did not increase with age, perhaps because of the decrease in total number of parietal cells. Hence, the age of onset of histologic gastritis largely coincided with onset of gastric H^+ secretion in *Cldn18*$^{-/-}$ stomach, suggesting a causal relationship between H^+ secretion and gastritis.

We next examined the levels of inflammation markers at postnatal days 1, 2, 3, and 4 (Figure 6*A*). Beginning at postnatal day 3, IL-1β in *Cldn18*$^{-/-}$ stomach was significantly and constantly up-regulated compared with *Cldn18*$^{+/+}$ (Figure 6). KC was also up-regulated, which was consistent with the neutrophil infiltration associated with *Cldn18*$^{-/-}$ gastritis in infant mice. COX-2 expression changed over the same time course as IL-1β, suggesting that prostaglandin E_2-related inflammation/restoration reactions occurred while IL-1β was up-regulated. Expression levels of TNF-α and MCP-1 tended toward later up-regulation (approximately postnatal day 14), consistent with the inflammation reaction. Markers such as IL-2 and IL-4 were not significantly up-regulated at postnatal days 3 and 4 (data not shown).

Together, these findings point to a role for claudin-18 in forming the H^+-resistant paracellular barrier between stomach epithelial cells and indicate that the barrier prevents gastritis by resisting inflammation. Consequently, defects in the H^+-resistant paracellular barrier caused by deleting claudin-18 result in inflammation induced due to

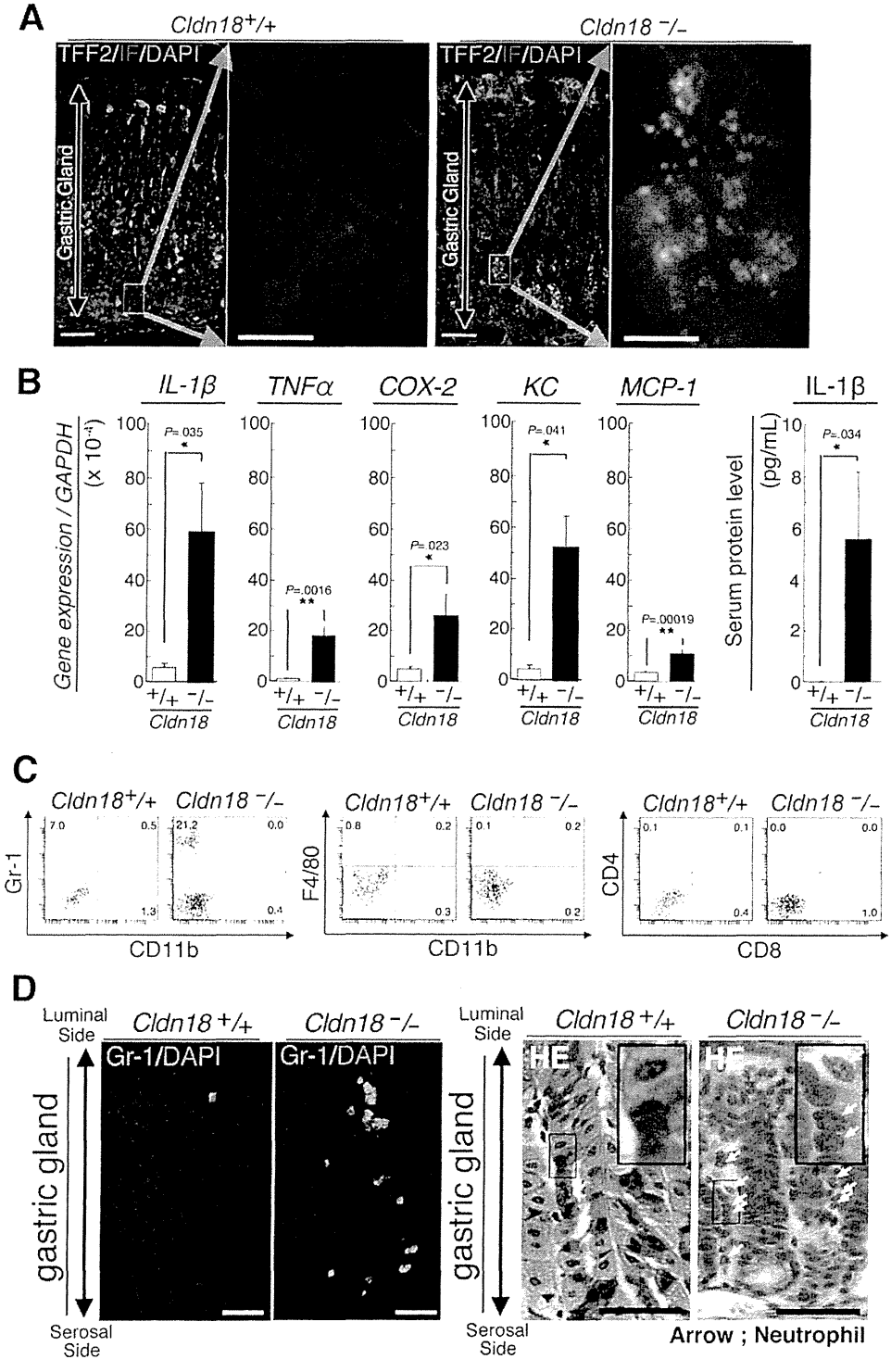

Figure 4. Characterization of the gastritis in *Cldn18*$^{-/-}$ mice. (*A*) Immunofluorescence images of sections stained for TFF2 and IF at low and high magnifications, respectively, in *Cldn18*$^{+/+}$ and *Cldn18*$^{-/-}$ adult stomach. *Bars* = 20 μm. (*B*) Expressions of inflammatory cytokines such as IL-1β, TNF-α, COX2, and KC were up-regulated in *Cldn18*$^{-/-}$ stomach. n ≧ 4. (*C*) Fluorescence-activated cell sorter analysis of immune cell types in gastritic *Cldn18*$^{-/-}$ tissue. Neutrophils, which are positive for Gr-1 and negative for CD11b, were the dominant immune cell type. (*D*) Immunofluorescence micrographs for Gr-1– and H&E-stained micrographs. (*Insets*) High-power micrographs reveal infiltration of neutrophils. *Bars* = 50 μm.

the chronic recruitment of neutrophils and prostaglandin-related reactions.

Effects of Manipulating Gastric Acidity

To obtain additional evidence for or against our interpretation that gastritis in *Cldn18*$^{-/-}$ mice was caused by a paracellular leak of stomach gastric acid, we next examined the effects of administering hydrochloric acid at low concentration or omeprazole sodium, an inhibitor of H^+,K^+-ATPase, on the incidence of gastritis in *Cldn18*$^{+/+}$ and *Cldn18*$^{-/-}$ stomach (Figure 6*B* and *C*).

A low concentration of hydrochloric acid was given to *Cldn18*$^{+/+}$ and *Cldn18*$^{-/-}$ mice on postnatal day 1, when parietal cells have not yet differentiated. Although no

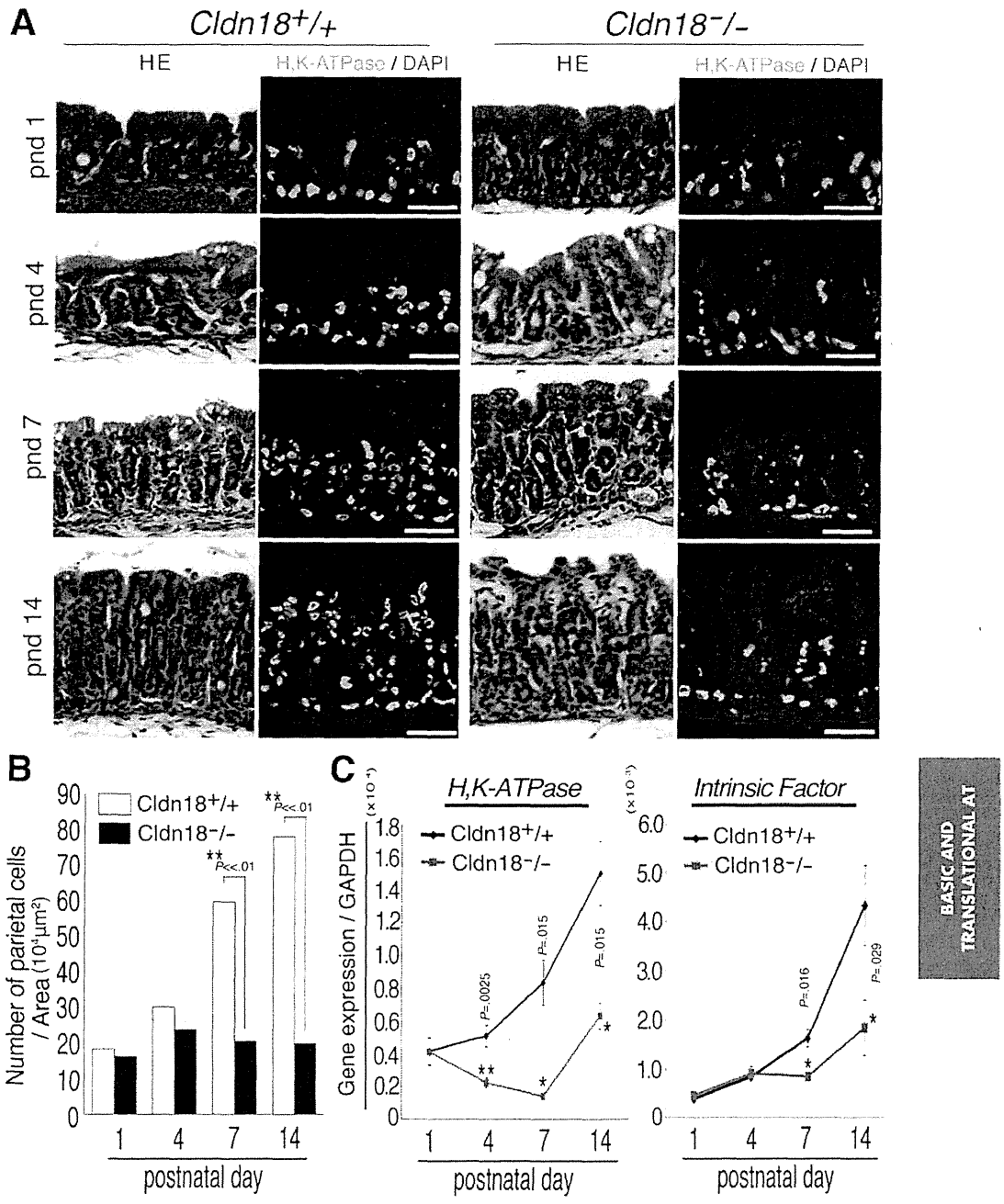

Figure 5. Age-related changes in *Cldn18*$^{+/+}$ and *Cldn18*$^{-/-}$ stomach. (*A*) Light microscopic images of H&E-stained paraffin sections and immunofluorescence micrographs stained for H^+,K^+-ATPase (H,K-ATPase) from *Cldn18*$^{+/+}$ and *Cldn18*$^{-/-}$ stomach at various times after birth. *Bars* = 50 μm. (*B*) Quantification of parietal cell number (shown as numbers per tissue area) in *Cldn18*$^{+/+}$ and *Cldn18*$^{-/-}$ stomach at different ages. (*C*) Gene expression level of markers for the differentiation of gastric cells. n ≧ 4.

inflammation was detected in mice given a neutral buffer, *Cldn18*$^{-/-}$ mice given hydrochloric acid showed stomach inflammation on postnatal day 2, as shown by IL-1β and COX2 levels (Figure 6*B*). When omeprazole was administered for 2 weeks starting at birth (twice a day with 5% dextrose in water), the expression of IL-1β in *Cldn18*$^{-/-}$ mice decreased to ~30% of that in untreated mice (Figure 6*C* [*i*]). The number of parietal cells at postnatal day 14 was significantly recovered by 14-day administration of omeprazole, at least partly indicative of decreased parietal cells after differentiation (Figure 6*C* [*ii*]). However, the induction of gastritis was not blocked, suggesting that omeprazole did not completely inhibit the secretion of gastric acid. These findings further support the idea that stomach acidity in *Cldn18*$^{-/-}$ mice triggers inflammation, which in turn induces gastritis.

Decrease in the Paracellular Barrier Function of Gastric Epithelial Cell Sheets on Claudin-18 Deficiency

We next examined the epithelial paracellular barrier function against H^+ in *Cldn18*$^{+/+}$ and *Cldn18*$^{-/-}$ stomach (Figure 7). Electrophysiologic measurements showed that total conductance was higher in *Cldn18*$^{-/-}$ stomach than *Cldn18*$^{+/+}$ stomach, suggesting that the claudin-18 deficiency resulted in defects in the paracellular barrier. In the

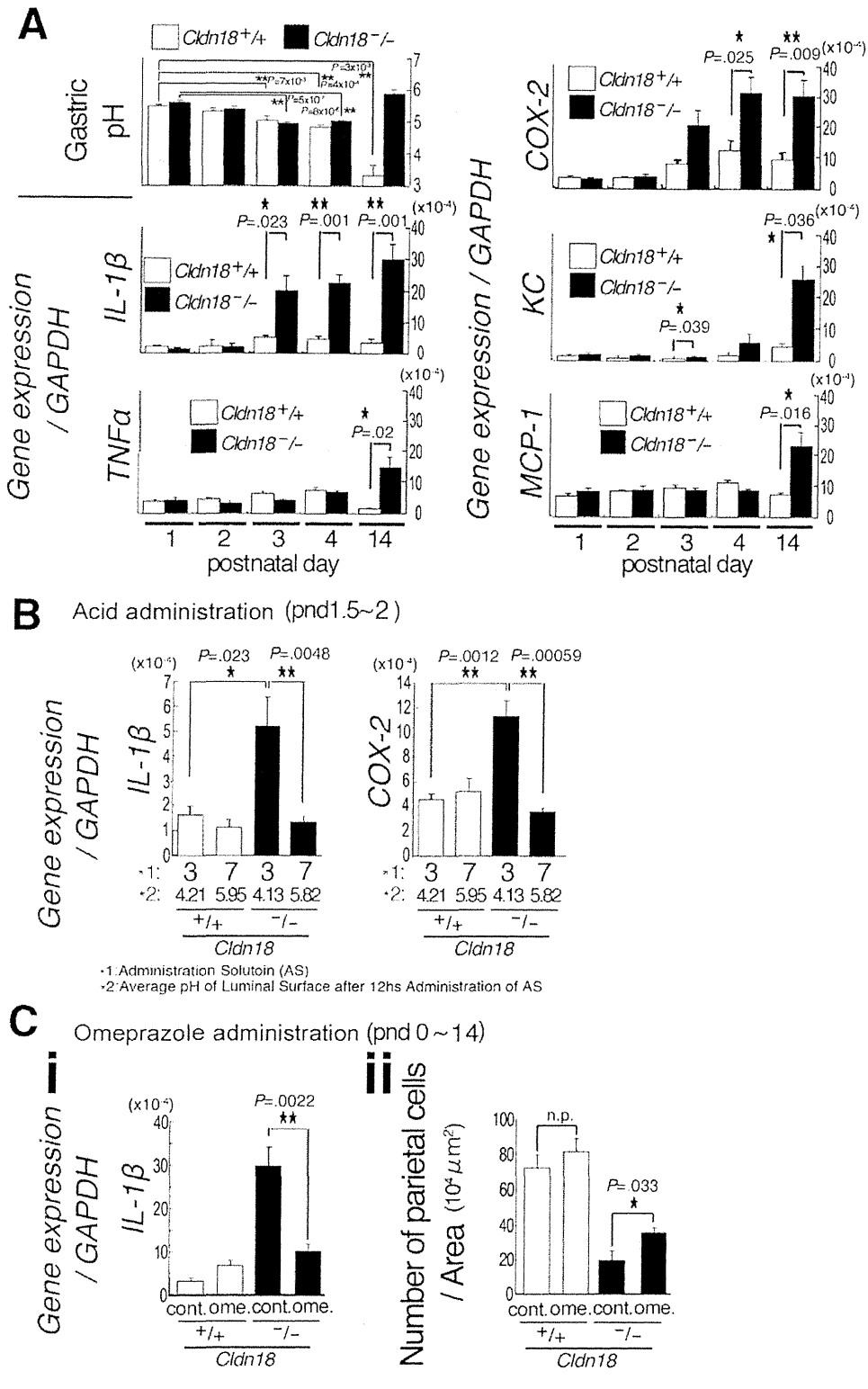

Figure 6. Onset of gastritis in *Cldn18*$^{+/+}$ and *Cldn18*$^{-/-}$ mice. (*A*) Time-dependent changes in pH and expression levels of IL-1β, TNF-α, COX-2, KC, and MCP-1 in untreated *Cldn18*$^{+/+}$ and *Cldn18*$^{-/-}$ mice. n ≧ 4. (*B*) IL-1β and COX-2 were up-regulated after oral administration of acid on postnatal day 1 in *Cldn18*$^{-/-}$ but not *Cldn18*$^{+/+}$ stomach. n ≧ 5. (*C* [*i*]) IL-1β was down-regulated following administration of the proton pump inhibitor omeprazole in *Cldn18*$^{-/-}$ but not *Cldn18*$^{+/+}$ stomach. n ≧ 5. (*C* [*ii*]) Quantification of parietal cell number (shown as numbers per tissue area) in *Cldn18*$^{+/+}$ and *Cldn18*$^{-/-}$ stomach with or without administration of omeprazole. Note that the number is partially recovered by omeprazole.

Cldn18$^{+/+}$ stomach, the paracellular barrier was sensitive to acidity, which caused the conductance to decrease, as shown by the Gt ratio (see Supplementary Materials and Methods) (Figure 7*A*). Consistent with this observation, we detected an H^+ leak by H^+ titration in infant mice, which was quite low in the *Cldn18*$^{+/+}$ stomach compared with the *Cldn18*$^{-/-}$ stomach (Figure 7*A*). In sharp contrast, in the *Cldn18*$^{-/-}$ stomach, the paracellular barrier was not sensitive to the acidity and showed a significantly higher H^+ leak compared with the *Cldn18*$^{+/+}$ stomach, as shown by the net proton flux

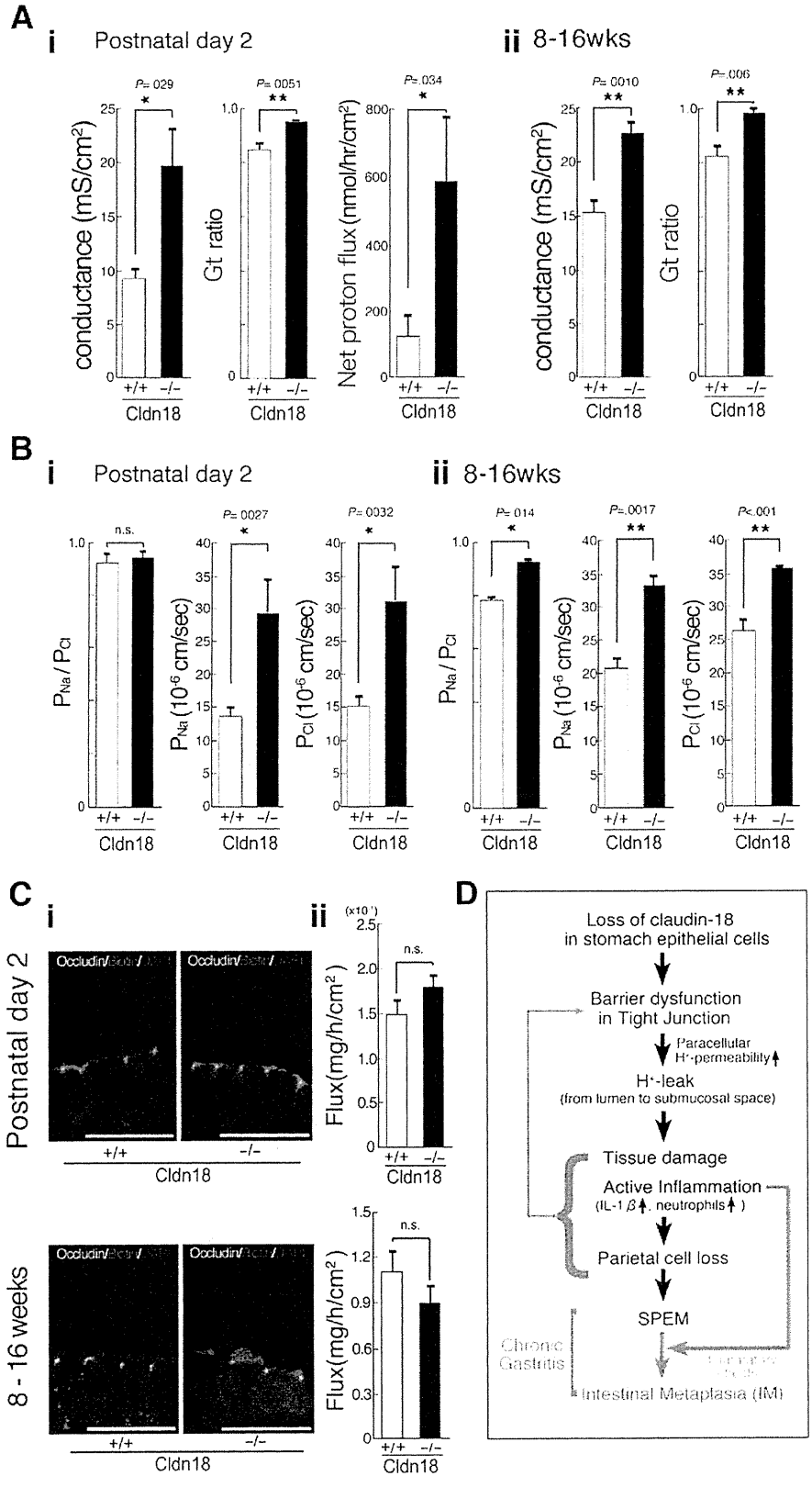

Figure 7. Paracellular permeability of H^+, Na^+, Cl^-, biotin, and dextran. (*A*) Transepithelial conductance and paracellular H^+ permeability at postnatal day 2 and 8–16 weeks in *Cldn18*$^{+/+}$ and *Cldn18*$^{-/-}$ stomach. H^+ permeability was sensitive to the addition of H^+ in *Cldn18*$^{-/-}$ but not in *Cldn18*$^{+/+}$ stomach. n ≧ 4. (*B*) Paracellular permeability of Na^+ and Cl^- in *Cldn18*$^{-/+}$ and *Cldn18*$^{-/-}$ stomach at postnatal day 2 and at 8–16 weeks. n ≧ 4. (*C*) The paracellular barrier to biotin and 4-kilodalton fluorescein isothiocyanate/dextran in *Cldn18*$^{-/-}$ and *Cldn18*$^{+/+}$ stomach in infants (postnatal day 2 of age) and adults (8–16 weeks of age). *Bars* = 20 μm (*D*) Schematic drawing of the pathologic changes of atrophic gastritis in *Cldn18*$^{-/-}$ mice.

(Figure 7*A*). These findings were consistent with the *Cldn18*$^{+/+}$ paracellular barrier in the stomach, providing a specific barrier against H^+ leakage.

On the other hand, dilution potential measurements for NaCl revealed that the paracellular permeability for Na^+ and Cl^- was higher in *Cldn18*$^{-/-}$ mice, even though the ratios of the permeabilities for Na^+ and Cl^- for adult and infant *Cldn18*$^{+/+}$ and *Cldn18*$^{-/-}$ stomachs were similar (0.8–0.95) (Figure 7*B*). Furthermore, no biotin (mol wt, 443 daltons) leakage was detected in either *Cldn18*$^{+/+}$ and *Cldn18*$^{-/-}$ mice, suggesting that pepsin leakage was not a major feature of the *Cldn18*$^{-/-}$-induced gastritis. As a measure of larger-sized molecules permeability, we measured the flux of 4-kilodalton dextran in the stomach of mice at postnatal day 2 and age 8–16 weeks, finding no differences between *Cldn18*$^{-/-}$ and *Cldn18*$^{+/+}$ stomachs (Figure 7*C*). These findings suggested that the *Cldn18*$^{-/-}$ stomach paracellular barrier was generally more leaky for ions than that of *Cldn18*$^{+/+}$ stomach, but not for larger-sized molecules, and that H^+ leakage due to the weak paracellular barrier in *Cldn18*$^{-/-}$ stomach was particularly important for the incidence of gastritis (Figure 7*D*).

Discussion

Atrophic gastritis is generally considered a high-risk condition for gastric cancer because of the accompanying metaplasia and dysplasia. Thus, identifying its causes is an important issue for anticancer therapy as well for maintaining a healthy gastric system. The stomach has several defense mechanisms to protect gastric epithelial tissue from various noxious materials, such as gastric acid and pepsin, and from stimulation by food. An imbalance between protection and insult can lead to gastritis. However, the way in which the TJ achieves its protective function is poorly understood.

A previous report and our present findings show that in atrophic gastritis and gastric cancer, the expression level of stomach-type claudin-18 is significantly decreased in human tissue, implicating claudin-18, directly or indirectly, in these pathological changes.[40] Our *Cldn18*$^{-/-}$ mice described here made a novel model of gastritis that can show the specific role of claudin-18 in the physiology and pathology of stomach epithelial barrier functions (Figure 7).

Of the two types of claudin-18, lung type and stomach type, stomach-type claudin-18 is the predominantly expressed variant in the stomach. Our present findings suggest paracellular barrier leakage of H^+ may be the primary cause of gastritis in *Cldn18*$^{-/-}$ mice. Additionally, in *Cldn18*$^{-/-}$ mice stomach, claudin-2 expression was slightly up-regulated and the Na^+ gradient facilitated Na^+ ions to pass from the submucosa to the gastric luminal space. As a result, H^+ could easily permeate the opposite direction. This H^+ leakage was associated with the up-regulation of proinflammatory cytokines, including IL-1β and COX-2, in our acid administration experiments and over the time course of development of gastritis, although the causal relationship between H^+ leakage and parietal cell differentiation could not be fully established.

There was also a slight change in gastric luminal pH due to a substantial change in the H^+ concentration. This led to metaplasia, an effect that omeprazole could partially inhibit. Other reports on metaplasia in the context of gastritis that have used *Helicobacter felis*-infected mice, histamine receptor knockout mice, occludin knockout mice, and Ménétrier disease models of transforming growth factor α overexpression mice indicate that it may be, at least partly, related to defects in barrier functions, although no direct association was shown.[42–44] In this respect, the expression level of occludin decreased in the superficial mucous epithelial cells of adult but not infant *Cldn18*$^{-/-}$ stomach, suggesting the possibility that the decreased expression of occludin may not contribute to the onset of gastritis but does contribute to its progression in *Cldn18*$^{-/-}$ stomach. Although the tissue differentiation caused by metaplasia is sensitive to numerous factors such as DMP-777, Hip1r KO, KLF4 KO, RUNX3 KO, K19-C2mE, and amphiregulin,[45–49] this report is the first to show a role for tight junctional claudins.

Although the level of IL-1β was significantly lower in *Cldn18*$^{-/-}$ mice seen here than in IL-1β transgenic mice from another study, it may still have been sufficient to trigger inflammation.[50] In those IL-1β–expressing transgenic mice, gastritis progresses to gastric cancer and splenectasis, which we did not detect at least in <20 weeks old *Cldn18*$^{-/-}$ mice. Considering that the rate of gastric cancer in the IL-1β–expressing transgenic mice depends on their IL-1β level, the absence of gastric cancer in our *Cldn18*$^{-/-}$ mice may be owing to the relatively low level of IL-1β. In addition, it was reported that transgenic mice expressing both COX-2 and prostaglandin E synthase 1 develop hyperplastic gastric tumors in which TNF-α plays an important role.[49] We then suggest that the down-regulation of claudin-18 leads to the basic conditions required for the progression of metaplasia. For dysplasia and neoplasia to occur in our *Cldn18*$^{-/-}$ mice, an additional risk factor that increases the level of cytokines such as IL-1β, COX-2, or TNF-α is needed. Future studies of metaplasia in *Cldn18*$^{-/-}$ mice should resolve this question.

The immune response in *Cldn18*$^{-/-}$ mice involves prominent infiltration of neutrophils into the inflamed regions. Given that IL-2, IL-4, and IL-6 were not up-regulated in these mice, however, T cells and B cells are probably not involved in the observed gastritis. The chronic recruitment of neutrophils in the *Cldn18*$^{-/-}$-related gastritis is in sharp contrast to the immune cell behavior in *H pylori*-induced and nonsteroidal anti-inflammatory drug–induced gastritis, in which the levels of biomarkers for Th1 cells, macrophages, and neutrophils all increased.[13,51] Therefore, it is possible that if the decreased claudin-18 level were combined with an additional risk factor that recruits T cells and B cells, the risk of dysplasia and neoplasia might increase greatly.

The role of paracellular barrier-forming claudins in inflammation is particularly noteworthy, because paracellular H^+ leakage may play a role in other kinds of chronic gastritis, including *H pylori*-induced gastritis. Along these lines, the loss of JAM-A, a TJ component, was reported to induce paracellular permeability and an increased susceptibility to dextran sulfate sodium-induced colitis.[52,53] Similar abnormalities are associated with other insults to paracellular barrier function. Because the paracellular barrier shows great variability in its molecular constitution and barrier function, multiple molecular mechanisms can probably lead to inflammation under a variety of conditions. Here we show that claudin-18–dependent formation of the paracellular barrier against H^+ diffusion is likely to play a specific role in prevention of gastritis. As more studies on claudin knockout mice are published, better understanding of its specific physiologic and pathologic functions, especially with regard to inflammation, will emerge, potentially leading to new therapeutic strategies against epithelial barrier-related diseases.

Supplementary Material

Note: To access the supplementary material accompanying this article, visit the online version of *Gastroenterology* at www.gastrojournal.org, and at doi: 10.1053/j.gastro.2011.10.040.

References

1. Cario E. Heads up! How the intestinal epithelium safeguards mucosal barrier immunity through the inflammasome and beyond. Curr Opin Gastroenterol 2010;26:583–590.
2. Marchiando AM, Graham WV, Turner JR. Epithelial barriers in homeostasis and disease. Annu Rev Pathol 2010;5:119–144.
3. Tsukita S, Furuse M, Itoh M. Multifunctional strands in tight junctions. Nat Rev Mol Cell Biol 2001;2:285–293.
4. Van Itallie CM, Anderson JM. Claudins and epithelial paracellular transport. Annu Rev Physiol 2006;68:403–429.
5. Gupta IR, Ryan AK. Claudins: unlocking the code to tight junction function during embryogenesis and in disease. Clin Genet 2010; 77:314–325.
6. Powell DW. Barrier function of epithelia. Am J Physiol 1981;241: G275–G288.
7. Claude P, Goodenough DA. Fracture faces of zonulae occludentes from "tight" and "leaky" epithelia. J Cell Biol 1973;58:390–400.
8. Laine L, Takeuchi K, Tarnawski A. Gastric mucosal defense and cytoprotection: bench to bedside. Gastroenterology 2008;135: 41–60.
9. Weis VG, Goldenring JR. Current understanding of SPEM and its standing in the preneoplastic process. Gastric Cancer 2009;12: 189–197.
10. Mills JC, Shivdasani RA. Gastric epithelial stem cells. Gastroenterology 2011;140:412–424.
11. Ohnishi N, Yuasa H, Tanaka S, et al. Transgenic expression of *Helicobacter pylori* CagA induces gastrointestinal and hematopoietic neoplasms in mouse. Proc Natl Acad Sci U S A 2008;105: 1003–1008.
12. Srivastava A, Lauwers GY. Pathology of non-infective gastritis. Histopathology 2007;50:15–29.
13. Becker JC, Domschke W, Pohle T. Current approaches to prevent NSAID-induced gastropathy—COX selectivity and beyond. Br J Clin Pharmacol 2004;58:587–600.
14. Oshima H, Hioki K, Popivanova BK, et al. Prostaglandin E_2 signaling and bacterial infection recruit tumor-promoting macrophages to mouse gastric tumors. Gastroenterology 2011;140:596–607.
15. Ishihara S, Fukuda R, Fukumoto S. Cytokine gene expression in the gastric mucosa: its role in chronic gastritis. J Gastroenterol 1996;31:485–490.
16. Lin WW, Karin M. A cytokine-mediated link between innate immunity, inflammation, and cancer. J Clin Invest 2007;117:1175–1183.
17. Sanders MJ, Ayalon A, Roll M, et al. The apical surface of canine chief cell monolayers resists H+ back-diffusion. Nature 1985; 313:52–54.
18. Chen MC, Chang A, Buhl T, et al. Apical acidification induces paracellular injury in canine gastric mucosal monolayers. Am J Physiol 1994;267:G1012–G1020.
19. Jovov B, Van Itallie CM, Shaheen NJ, et al. Claudin-18: a dominant tight junction protein in Barrett's esophagus and likely contributor to its acid resistance. Am J Physiol Gastrointest Liver Physiol 2007;293:G1106–G1113.
20. Madara JL. Regulation of the movement of solutes across tight junctions. Annu Rev Physiol 1998;60:143–159.
21. Umeda K, Ikenouchi J, Katahira-Tayama S, et al. ZO-1 and ZO-2 independently determine where claudins are polymerized in tight-junction strand formation. Cell 2006;126:741–754.
22. Guillemot L, Paschoud S, Pulimeno P, et al. The cytoplasmic plaque of tight junctions: a scaffolding and signalling center. Biochim Biophys Acta 2008;1778:601–613.
23. Balda MS, Matter K. Tight junctions and the regulation of gene expression. Biochim Biophys Acta 2009;1788:761–767.
24. Bauer HC, Traweger A, Zweimueller-Mayer J, et al. New aspects of the molecular constituents of tissue barriers. J Neural Transm 2011;118:7–21.
25. Furuse M, Fujita K, Hiiragi T, et al. Claudin-1 and -2: novel integral membrane proteins localizing at tight junctions with no sequence similarity to occludin. J Cell Biol 1998;141:1539–1550.
26. Van Itallie CM, Fanning AS, Anderson JM. Reversal of charge selectivity in cation or anion-selective epithelial lines by expression of different claudins. Am J Physiol Renal Physiol 2003;285: F1078–F1084.
27. Mineta K, Yamamoto Y, Yamazaki Y, et al. Predicted expansion of the claudin multigene family. FEBS Lett 2011;585:606–612.
28. Simon DB, Lu Y, Choate KA, et al. Paracellin-1, a renal tight junction protein required for paracellular Mg2+ resorption. Science 1999;285:103–106.
29. Muto S, Hata M, Taniguchi J, et al. Claudin-2-deficient mice are defective in the leaky and cation-selective paracellular permeability properties of renal proximal tubules. Proc Natl Acad Sci U S A 2010;107:8011–8016.
30. Tamura A, Hayashi H, Imasato M, et al. Loss of claudin-15, but not claudin-2, causes Na+ deficiency and glucose malabsorption in mouse small intestine. Gastroenterology 2011;140:913–923.
31. Morita K, Furuse M, Fujimoto K, et al. Claudin multigene family encoding four-transmembrane domain protein components of tight junction strands. Proc Natl Acad Sci U S A 1999;96:511–516.
32. Niimi T, Nagashima K, Ward JM, et al. Claudin-18, a novel downstream target gene for the T/EBP/NKX2.1 homeodomain transcription factor, encodes lung- and stomach-specific isoforms through alternative splicing. Mol Cell Biol 2001;21:7380–7390.
33. Tamura A, Kitano Y, Hata M, et al. Megaintestine in claudin-15-deficient mice. Gastroenterology 2008;134:523–534.
34. Tamura A, Kikuchi S, Hata M, et al. Achlorhydria by ezrin knockdown: defects in the formation/expansion of apical canaliculi in gastric parietal cells. J Cell Biol 2005;169:21–28.
35. Matsubayashi M, Ando H, Kimata I, et al. Effect of low pH on the morphology and viability of Cryptosporidium andersoni sporozoites and histopathology in the stomachs of infected mice. Int J Parasitol 2011;41:287–292.

36. Shao J, Sartor RB, Dial E, et al. Expression of intrinsic factor in rat and murine gastric mucosal cell lineages is modified by inflammation. Am J Pathol 2000;157:1197–1205.
37. Huh WJ, Esen E, Geahlen JH, et al. XBP1 controls maturation of gastric zymogenic cells by induction of MIST1 and expansion of the rough endoplasmic reticulum. Gastroenterology 2010;139:2038–2049.
38. Angelow S, Kim KJ, Yu AS. Claudin-8 modulates paracellular permeability to acidic and basic ions in MDCK II cells. J Physiol 2006;571:15–26.
39. Drakes ML, Czinn SJ, Blanchard TG. Regulation of murine dendritic cell immune responses by Helicobacter felis antigen. Infect Immun 2006;74:4624–4633.
40. Sanada Y, Oue N, Mitani Y, et al. Down-regulation of the claudin-18 gene, identified through serial analysis of gene expression data analysis, in gastric cancer with an intestinal phenotype. J Pathol 2006;208:633–642.
41. Nozaki K, Ogawa M, Williams JA, et al. A molecular signature of gastric metaplasia arising in response to acute parietal cell loss. Gastroenterology 2008;134:511–522.
42. Takagi H, Jhappan C, Sharp R, et al. Hypertrophic gastropathy resembling Ménétrier's disease in transgenic mice overexpressing transforming growth factor alpha in the stomach. J Clin Invest 1992;90:1161–1167.
43. Ogawa T, Maeda K, Tonai S, et al. Utilization of knockout mice to examine the potential role of gastric histamine H2-receptors in Menetrier's disease. J Pharmacol Sci 2003;91:61–70.
44. Saitou M, Furuse M, Sasaki H, et al. Complex phenotype of mice lacking occludin, a component of tight junction strands. Mol Biol Cell 2000;11:4131–4142.
45. Goldenring JR, Nomura S. Differentiation of the gastric mucosa III. Animal models of oxyntic atrophy and metaplasia. Am J Physiol Gastrointest Liver Physiol 2006:G999–G1004.
46. Keeley TM, Samuelson LC. Cytodifferentiation of the postnatal mouse stomach in normal and Huntingtin-interacting protein 1-related-deficient mice. Am J Physiol Gastrointest Liver Physiol 2010; 299:G1241–G1251.
47. Li QL, Ito K, Sakakura C, et al. Causal relationship between the loss of RUNX3 expression and gastric cancer. Cell 2002;109:113–124.
48. Nam KT, Lee HJ, Mok H, et al. Amphiregulin-deficient mice develop spasmolytic polypeptide expressing metaplasia and intestinal metaplasia. Gastroenterology 2009;136:1288–1296.
49. Oshima M, Oshima H, Matsunaga A, et al. Hyperplastic gastric tumors with spasmolytic polypeptide-expressing metaplasia caused by tumor necrosis factor-alpha-dependent inflammation in cyclooxygenase-2/microsomal prostaglandin E synthase-1 transgenic mice. Cancer Res 2005;65:9147–9151.
50. Tu S, Bhagat G, Cui G, et al. Overexpression of interleukin-1beta induces gastric inflammation and cancer and mobilizes myeloid-derived suppressor cells in mice. Cancer Cell 2008;14:408–419.
51. Amedei A, Cappon A, Codolo G, et al. The neutrophil-activating protein of Helicobacter pylori promotes Th1 immune responses. J Clin Invest 2006;116:1092–1101.
52. Laukoetter MG, Nava P, Lee WY, et al. JAM-A regulates permeability and inflammation in the intestine in vivo. J Exp Med 2007; 204:3067–3076.
53. Vetrano S, Rescigno M, Cera MR, et al. Unique role of junctional adhesion molecule-a in maintaining mucosal homeostasis in inflammatory bowel disease. Gastroenterology 2008; 135:173–184.

Received June 28, 2011. Accepted October 26, 2011.

Reprint requests

Address requests for reprints to: Sachiko Tsukita, PhD, Laboratory of Biological Science, Graduate School of Frontier Biosciences, Osaka University, 2-2 Yamadaoka, Suita, Osaka 565-0871, Japan. e-mail: atsukita@biosci.med.osaka-u.ac.jp; fax: (81) 6-6879-3329.

Acknowledgments

D.H. and A.T. contributed equally to this report.

The authors thank Drs J. Mills, D. Alpers, and M.Takeichi for their generous gifts of the antibodies; Drs M. Hatakeyama, T. Noda, E. Morii, and K. Aozasa for their helpful discussions; Dr M. Okabe and Ms K. Kawata for generating the claudin-18 knockout mice; Ms Hagiwara for technical assistance; and members of our laboratory for helpful discussion.

Conflicts of interest

The authors disclose no conflicts.

Funding

Supported in part by a Grant-in-Aid for Creative Scientific Research from the Ministry of Education, Science and Culture of Japan (to S.T.).

Ann Surg Oncol (2012) 19:1902–1910
DOI 10.1245/s10434-011-2175-4

Annals of
SURGICAL ONCOLOGY
OFFICIAL JOURNAL OF THE SOCIETY OF SURGICAL ONCOLOGY

ORIGINAL ARTICLE - THORACIC ONCOLOGY

Cytokeratin 7 is a Predictive Marker for Survival in Patients with Esophageal Squamous Cell Carcinoma

Naohide Oue, MD, PhD[1], Tsuyoshi Noguchi, MD, PhD[2], Katsuhiro Anami, MD, PhD[1], Seigo Kitano, MD, PhD[3], Naoya Sakamoto, MD, PhD[1], Kazuhiro Sentani, MD, PhD[1], Naohiro Uraoka, MD[1], Kazuhiko Aoyagi, PhD[4], Teruhiko Yoshida, MD[4], Hiroki Sasaki, PhD[4], and Wataru Yasui, MD, PhD[1]

[1]Department of Molecular Pathology, Hiroshima University Graduate School of Biomedical Sciences, Hiroshima, Japan; [2]Center for Community Medicine, Division of Surgery, Oita University Faculty of Medicine, Yufu, Japan; [3]Department of Surgery I, Oita University Faculty of Medicine, Yufu, Japan; [4]Division of Genetics, National Cancer Center Research Institute, Tokyo, Japan

ABSTRACT

Background. Patients diagnosed with stage II and III esophageal squamous cell carcinoma (ESCC) have variable prognosis. This group would benefit greatly from the discovery of prognostic markers that are capable of identifying individuals for whom adjuvant treatment would be advantageous. The aim of this study was to investigate the impact of immunohistochemically detected cytokeratin 7 (CK7) expression on disease-free survival, overall survival (OS), or therapeutic outcome in patients with ESCC.

Methods. Immunohistochemical analysis of CK7 was performed on 225 surgically resected specimens of stage 0–III ESCC.

Results. In total, 20 (9%) of 225 ESCC cases were positive for CK7. In stage 0–III ESCC patients, CK7 expression was statistically significantly associated with OS, independent of clinical covariates, including tumor, node, metastasis system stage. In stage II and III ESCC patients ($n = 124$), CK7 expression was significantly associated with poorer OS ($P = 0.0377$). Furthermore, in stage II and III ESCC patients who did not receive adjuvant chemotherapy ($n = 73$), CK7 expression was significantly associated with poorer OS ($P = 0.0003$). CK7 expression was not associated with therapeutic outcome in patients with stage II and III ESCC who received adjuvant chemotherapy. In patients with CK7-positive ESCC ($n = 16$), receipt of adjuvant chemotherapy tended to be beneficial for patients with stage II and III ESCC ($P = 0.0654$).

Conclusions. Immunohistochemical analysis of CK7 will help to identify high-risk patients.

Electronic supplementary material The online version of this article (doi:10.1245/s10434-011-2175-4) contains supplementary material, which is available to authorized users.

First Received: 19 July 2011;
Published Online: 28 December 2011

W. Yasui, MD, PhD
e-mail: wyasui@hiroshima-u.ac.jp

According to the World Health Organization, esophageal cancer is the sixth most common malignancy worldwide.[1] The two predominant forms of esophageal cancer are squamous cell carcinoma and adenocarcinoma. Globally, squamous cell carcinoma accounts for more than 90% of esophageal cancer. Most esophageal squamous cell carcinoma (ESCC) is diagnosed at an advanced stage, and even superficial ESCC that appears to extend no further than the submucosa metastasizes to the lymph nodes in 50% of cases.[2] For localized ESCC, surgery is the primary therapeutic option. However, the prognosis is unsatisfactory, even in curatively resected patients where the 5-year survival rate is <50% after surgery.[3] Several prognostic markers, such as nodal status and tumor stage, are currently accepted for clinical use, and we have previously reported several ESCC-associated genes.[4–7] However, these genes cannot completely identify which patients are at low or high risk for disease recurrence. Therefore, identification of novel prognostic markers for patients with ESCC is important.

Expression of the *KRT7* gene, which encodes cytokeratin 7 (CK7), has been identified by microarray analysis to be involved in the poor prognosis of ESCC patients.[8] CK7 is expressed in several simple ductal epithelia, in mesothelium, and in urothelium. However, CK7 is sparsely